FOG OCCURRENCE AND FORECASTING AT TWO NORTH PACIFIC OCEAN STATIONS, MAY AND JUNE, 1953

Frank John Misciasci

NPS-58MI74101

NAVAL POSTGRADUATE SCHOOL
Monterey, California

THESIS

FOG OCCURRENCE AND FORECASTING
AT TWO NORTH PACIFIC OCEAN
STATIONS, MAY AND JUNE, 1953

by

Frank John Misciasci, Jr.

September 1974

Thesis Advisor D. F. Leipper

Approved for public release; distribution unlimited.

Prepared for:
Naval Air Systems Command
Washington, D.C. 20360

Air Weather Service
Scott AFB, Illinois 62225

NAVAL POSTGRADUATE SCHOOL
Monterey, California

Rear Admiral Isham Linder
Superintendent

Jack R. Borsting
Provost

This thesis prepared in conjunction with research supported in part by Air Weather Service and in part by Naval Air Systems Command under PO 4-1027 issued 26 July 1973, and PO 5-1051 issued 18 June 1974.

SECURITY CLASSIFICATION OF THIS PAGE *(When Data Entered)*

REPORT DOCUMENTATION PAGE		READ INSTRUCTIONS BEFORE COMPLETING FORM
1. REPORT NUMBER NPS-58MI74101	2. GOVT ACCESSION NO.	3. RECIPIENT'S CATALOG NUMBER
4. TITLE *(and Subtitle)* Fog Occurrence and Forecasting at Two North Pacific Ocean Stations, May and June, 1953		5. TYPE OF REPORT & PERIOD COVERED Master's Thesis; September 1974 6. PERFORMING ORG. REPORT NUMBER
7. AUTHOR(s) Frank John Misciasci, Jr. In conjunction with Dale F. Leipper		8. CONTRACT OR GRANT NUMBER(s)
9. PERFORMING ORGANIZATION NAME AND ADDRESS Naval Postgraduate School Monterey, California 93940		10. PROGRAM ELEMENT, PROJECT, TASK AREA & WORK UNIT NUMBERS 62755N; PO4-1027 62759N; PO-5-1051
11. CONTROLLING OFFICE NAME AND ADDRESS Naval Air Systems Command Washington, DC 20360		12. REPORT DATE September 1974 13. NUMBER OF PAGES 111
14. MONITORING AGENCY NAME & ADDRESS*(if different from Controlling Office)*		15. SECURITY CLASS. *(of this report)* Unclassified 15a. DECLASSIFICATION/DOWNGRADING SCHEDULE

16. DISTRIBUTION STATEMENT *(of this Report)*

Approved for public release; distribution unlimited.

17. DISTRIBUTION STATEMENT *(of the abstract entered in Block 20, if different from Report)*

18. SUPPLEMENTARY NOTES

19. KEY WORDS *(Continue on reverse side if necessary and identify by block number)*

Fog, Forecasting, Inversion, Synoptic, Weather Ships, Visibility

20. ABSTRACT *(Continue on reverse side if necessary and identify by block number)*

The problem of forecasting marine fog in the North Pacific has been hampered by insufficient knowledge of meteorological parameters which are intrinsic to its formation.

Eight hundred ninety six observations at three-hourly intervals from two North Pacific Ocean Stations during May and June 1953 were analyzed. Fixed point time series analysis methods

DD FORM 1 JAN 73 1473 EDITION OF 1 NOV 65 IS OBSOLETE
S/N 0102-014-6601 |

Unclassified
SECURITY CLASSIFICATION OF THIS PAGE *(When Data Entered)*

were used for selected point parameters. Analyses of radiosonde data for the surface to the seven hundred fifty-millibar level provided information on the relationship between marine fog and the occurrence of low level inversions. Synoptic flow patterns were determined from surface pressure maps.

Results indicate that the dewpoint-sea surface temperature and the dewpoint-air temperature relations are critical to fog formation at these two stations and that fog formation is associated with certain specific flow patterns and inversion sequences. The duration of airmass fog was found to be related to the thickness of the associated inversion and to the duration of the exposure of the airmass to a cooling sea surface.

Fog Occurrence and Forecasting at Two North Pacific Ocean Stations, May and June, 1953

by

Frank John Misciasci, Jr.
Captain, United States Air Force
B.S., Ohio State University, 1969
B.S., University of Utah, 1970

Submitted in partial fulfillment of the
requirements for the degree of

MASTER OF SCIENCE IN OCEANOGRAPHY

from the

NAVAL POSTGRADUATE SCHOOL
September 1974

ABSTRACT

The problem of forecasting marine fog in the North Pacific has been hampered by insufficient knowledge of meteorological parameters which are intrinsic to its formation.

Eight hundred ninety six observations at three-hourly intervals from two North Pacific Ocean Stations during May and June 1953 were analyzed. Fixed point time series analysis methods were used for selected point parameters. Analyses of radiosonde data for the surface to the seven hundred fifty-millibar level provided information on the relationship between marine fog and the occurrence of low level inversions. Synoptic flow patterns were determined from surface pressure maps.

Results indicate that the dewpoint-sea surface temperature and the dewpoint-air temperature relations are critical to fog formation at these two stations and that fog formation is associated with certain specific flow patterns and inversion sequences. The duration of airmass fog was found to be related to the thickness of the associated inversion and to the duration of the exposure of the airmass to a cooling sea surface.

TABLE OF CONTENTS

LIST OF TABLES

LIST OF ILLUSTRATIONS

TABLE OF SYMBOLS AND ABBREVIATIONS

C.	Degrees Celsius
d()/dt	Rate of change of () with time
°F.	Degrees Fahrenheit
FT.	Feet
HRS.	Hours
KTS.	Knots
LCL	Local standard time
MB.	Millibar
nm	Nautical miles
OBS.	Observations
Q	Ocean Station Vessel Quebec
S	Ocean Station Vessel Sierra
R.H.	Relative humidity (percent)
Ta	Air temperature (C.)
Td	Dewpoint temperature (C.)
Tmi	Maximum sounding temperature (C.)
Tw, Tsst	Sea surface temperature (C.)
∇ Tw	Sea surface temperature gradient (C., F.)
V	Vector wind
Z	Zulu Time
∇ z	Change in height (feet)
<	Less than
>	Greater than

ACKNOWLEDGEMENT

The author wishes to express his appreciation to Dr. Dale F. Leipper of the Naval Postgraduate School for his many hours of guidance and encouragement during the course of this investigation, and to Professor Charles L. Taylor of the Naval Postgraduate School whose constructive comments aided in the completion of this paper.

In particular, the author wishes to thank his wife, without whose assistance and understanding this undertaking could not have been accomplished.

I. INTRODUCTION

Fogs which occur over open ocean areas present challenging problems in analysis and forecasting, not alone to meteorologists but to naval strategists, merchant mariners and fishermen as well. The economic and strategic consequences of oceanic fogs as well as their affect on aviation and carrier operations have been documented by Wheeler [20]. Given the importance of oceanic fog to naval operations it is apparent that the ability to reliably forecast the occurrence of such fogs is a necessary component of operational mission planning, both at sea and prior to sailing.

Byers [1] has defined fog in general as stratus cloud cover forming at, or near enough, to the ground so as to seriously affect surface visibility. A more specific classification system originally developed by Willet [21] and modified by Byers separates all fogs into either air-mass or frontal fogs. The former are characterized by a lowering of the air temperature while the latter are typified by an increase in the dewpoint temperature. The complete classification from Byers [1] is as follows:

A. Air-mass fogs

1. Advection types

a. Types due to the transport of warm air over a cold surface.

(1) Land- and sea-breeze fog

(2) Sea fog

(3) Tropical-air fog

b. Types due to the transport of cold air over a warm surface.

(1) Steam fogs (arctic "sea smoke")

2. Radiation types

a. Ground fog

b. High-inversion fog

3. Advection-radiation fog (radiation over land in damp sea air).

4. Upslope fogs (adiabatic-expansion fog)

B. Frontal fogs

1. Prefrontal (warm-front) fog

2. Postfrontal (cold-front) fog

3. Front-passage fog

Those which can occur over open ocean areas are:

1. The advection sea fogs, which result from the cooling of marine air over an ocean current,

2. Tropical air fogs, which result due to the cooling from below of air moving from low to higher latitudes across a sea surface temperature gradient, and

3. The frontal fogs.

The ability to forecast fog at a particular ocean location depends in part upon obtaining a description of the types of fog occurring at the location in question. The parameters involved in the formation of that particular fog must then be examined to determine their forecastability.

There are three main approaches which can be employed in the analysis and forecasting of oceanic fog. They are the climatological, the statistical-numerical and the synoptic.

The climatological approach consists of compiling all available observations at a given location or in a given area and determining the monthly, or seasonal averages of fog occurrence as well as the diurnal variability which may occur in any given mean case. The resultant product, simplified into atlas form such as the U.S. Navy Marine Climatic Atlas of the World [2] may give valuable insight into long range strategic planning considerations. A further example of the efficacy of this approach is the climatic compilation done by the Naval Weather Research Facility in 1962 [18]. This publication concerns specific probabilities of limiting parameters on carrier task force operation in the North Pacific. This approach, while not a direct forecast in itself, is a useful "first handle" in delineating areas in which fog forecasting must be considered in naval operational planning. It is also a necessary starting point for the two subsequent analysis techniques.

Statistical-numerical techniques in fog forecasting have been prominent only in recent years, since this method depends heavily upon the ability of computers to handle large data grids. A prime example of this approach is the method of regression analysis. Schramm [15] and Nelson [10] have employed this technique to obtain visibility equations, which are functions of linear combinations of constituent

parameters that influence the formation of fog and the resultant low visibilities which accompany fog formation. This technique has met with only limited success partly because it is dependent upon inputs from prognosticated temperature and humidity fields. The resultant products of current temperature and humidity forecasts over the ocean are not sufficiently accurate to be employed as inputs in a statistical scheme according to Nelson.

The synoptic approach to fog forecasting is a combination of climatology with the analysis of those factors inherent in the movement of individual airmasses across the ocean on a daily real time basis. The subjective analysis of individual fog occurrences is combined with the objective analysis of the relationship between surface wind trajectories, dewpoint and air temperature changes. The sea surface temperature gradient and surface pressure changes are also considered along with the overall synoptic scale pressure pattern to infer the likelihood and duration of fog at a particular location of interest.

This paper will adopt the synoptic approach to fog forecasting in an Eulerian framework by examining fog formations at two ocean stations in the North Pacific over a representative period of time.

II. BACKGROUND

A. PAST INVESTIGATION

Investigation of the occurrence of ocean fog has been hampered in the past by the lack of suitable surface and upper air data. Information on sea fog had been based primarily upon the observations made by transiting commercial and naval shipping. Specific efforts to obtain data for research have been few in number in the past. Perhaps the earliest and one of the best studies made of the problem was that of Taylor [17], who investigated the formation of fog in the Grand Banks off Newfoundland. Using thermodynamic measurements made from the whaler SCOTIA, and determining air trajectories from ship reports in the vicinity, Taylor demonstrated that these fogs were caused by air moving from warm waters across the cold currents in the Banks. This study formed the basis for the afore mentioned sea fog type.

Subsequent efforts have concentrated primarily upon the occurrence of coastal fogs, not surprising, considering that fixed point observations were readily available and that this phenomena occurs in areas which are heavily populated. Synoptic methods were applied to this type of fog by Leipper [7, 8] in 1948 and 1968, who investigated coastal fog formation in San Diego. Considering an analysis of the local flow together with local thermodynamic and sea surface temperature

conditions he determined indicies based on the height of the inversion base, the air-sea temperature difference, and the moisture level. These indicies have provided the basis for local forecasting efforts in the southern California coastal military communities.

An earlier study of summer fog at Shemya by Leipper [9] also employed the techniques of synoptic analysis to determine a local fog forecasting method for this phenomenon. This method involved the forecasting of temperature and dewpoint changes and a consideration of the sea surface temperature. Types of synoptic patterns which can result in fog formation were delineated.

Stevenson [16] made a study of fog occurrence along the Yorkshire coast in England and determined a forecasting scheme based upon wind velocity and direction, wind duration, air-water temperature difference, and air temperature-dewpoint difference. Again synoptic techniques were used to subdivide fog occurrence down to its causative parameters, and forecast these.

Grisham and Renard [4] employed a climatological-synoptic approach to oceanic fogs in the North Pacific by utilizing all available ship reports and climatological pressure pattern means in a single month to determine the distribution of fog about idealized synoptic pressure systems. An improved ocean fog climatology is the end result of this approach.

The existence of oceanic weather observation ships dating from 1940 provided semi-continuous data from specific locations

in the North Pacific and the North Atlantic. One such vessel, EXTRA, located east of Japan along the North wall of the Kuroshio at 39° N and 153° W, provided the basis for a synoptic study of the occurrence of sea fog at this location. Ogata and Tamura [12] and Ogata, Kanazawa, and Yoshida [11] investigated the relationship of the synoptic pressure patterns, sea surface temperature isotherms, air-sea temperature difference, wind direction and velocity, and radiosonde temperature soundings to the occurrence of sea fog at EXTRA. Six synoptic circulation types were identified as being accompanied by fog or drizzle at the station, three with Northerly and three with Southerly flow. Although no attempt was made to specifically forecast fog, the Japanese studies showed that an examination of fixed ship data could be utilized to determine synoptic conditions favorable for the formation of sea fog at that point.

B. PRESENT STATUS

The U.S. Weather Service currently forecasts the occurrence of oceanic fog by a climatological-synoptic approach. The emphasis is on forecasting Tropical air type fog and the indicies used include a study of the wind field, upstream moisture conditions for the area of interest, and synoptic surface pressure pattern movements.

The U.S. Naval Fleet Numerical Weather Central (FNWC) in Monterey, California, provides an objective fog forecast

based on a statistical computer analysis of various parameters which are either products of computer analyses or Primitive Equation prognosis. These parameters consist of air temperature, evaporation, condensation, relative humidity, geostrophic thermal advection, and horizontal mixing. The primary use of this product is in the Optimum Ship Track Routing (OTSR) program provided by FNWC to Naval and government contract shipping. The forecast itself takes the form of a probability of occurrence. According to Renard [13], use of this product is limited and the accuracy is not believed to be at an operationally acceptable level.

At the present time, these are the only U.S. agencies actively engaged in oceanic fog forecasting.

III. APPROACH

A. DATA SELECTION

The Eulerian approach to meteorological analysis, i.e. the examination of the changes in meteorological parameters at a fixed location with time, has been employed since fixed point observations began. The efficacy of this approach when combined with synoptic scale analysis has been demonstrated in forecast studies at virtually every military and civilian land forecast center.

One problem of analyzing the occurrence of oceanic fog has been that, unlike the land, there is no fixed dense network of weather observations at sea. The Fixed Ocean Station Vessel (OSV) program begun in the late 1940's in both the Atlantic and Pacific Oceans was the closest approach to such a network. U.S. Coast Guard vessels were employed as fixed location weather observation platforms and the positions of those O.S.V. stations located in the Pacific are shown in Figure 1. Although some of these stations existed for only a few years, many observations were compiled. When an Eulerian analysis of the synoptic occurrence of fog was decided upon, the availability of this data was examined. The Ocean Station Vessel observations are maintained on microfilm at the United States Climatic Center in Asheville, North Carolina.

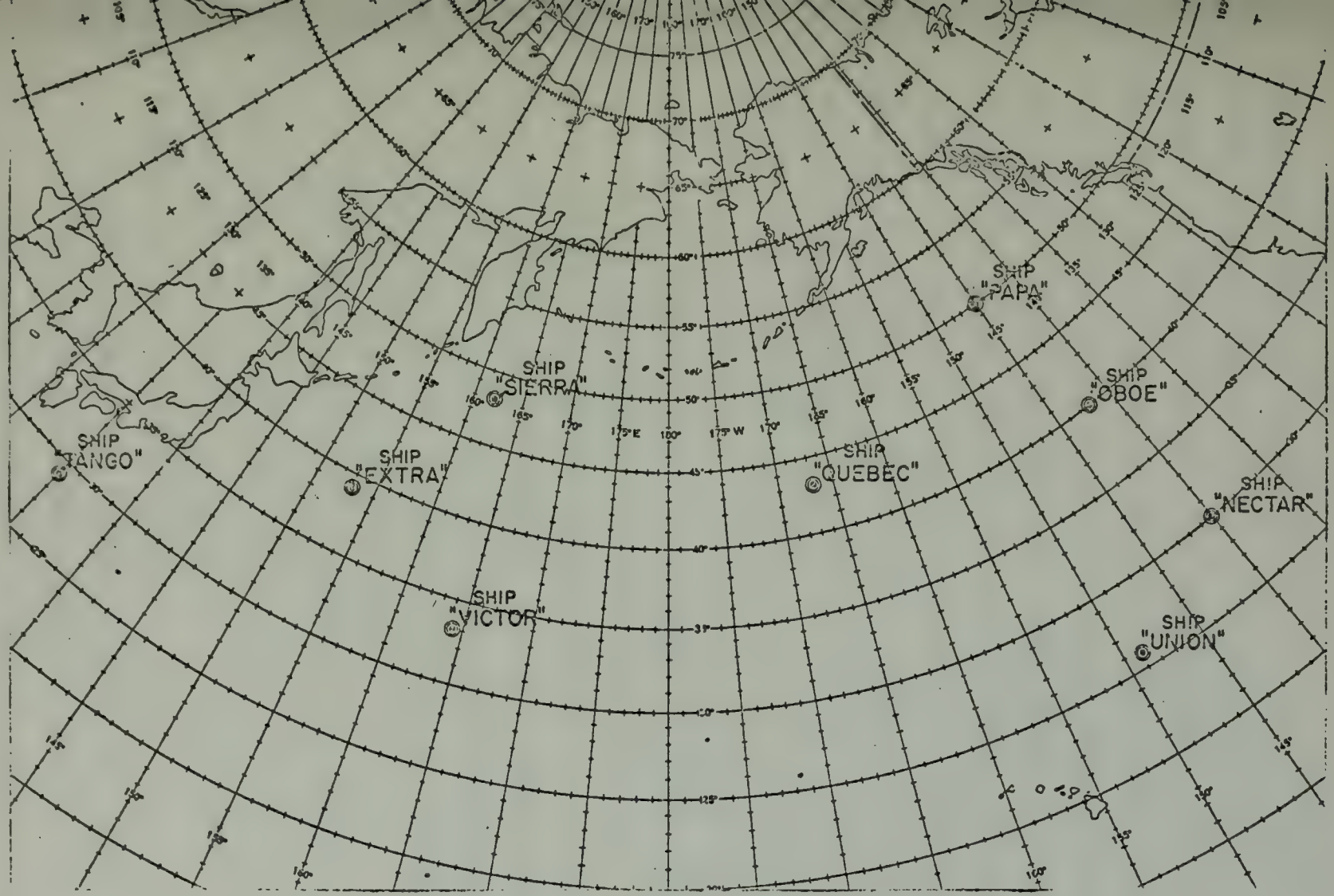

NORTH PACIFIC O.S.V. LOCATIONS (After [18])

FIGURE 1

Reference to existing climatologies [2] with regard to high probability of fog occurrence in the North Pacific areas revealed that two O.S.V. stations, QUEBEC (Q) and SIERRA (S) were located in the area of maximum fog occurrence. Station QUEBEC was an open ocean station located at 43°N 167°W, 660 nm due south of Dutch Harbor Alaska, well removed from land mass influence. Station SIERRA, on the other hand, was located at 48°N 162°E, 275 nm southeast of the tip of the Kamchatka Peninsula and 400 nm due east of the Kurile Islands. The relative proximity of Station S to land mass areas figured in its choice as a station to be analyzed, since it provides a contrast to ship station Q insofar as oceanographic considerations are concerned. Figure 2 shows the position of these stations relative to the main circulation of the currents of the North Pacific. It can be observed that S is located in the area of the Oyashio current, and just north of the zone of confluence between the Oyashio and the Kuroshio current coming up from the South. Station Q, however, lies astride the North Pacific Drift.

All observations taken by these two O.S.V.'s during the years 1950 - 1953 were requested and received on microfilm from the Climatic Center. These observations included the following information:

1. Station synoptic weather observations taken at three-hour intervals including surface wind, air temperature, dewpoint, sea level pressure, visibility, ceiling and sea surface temperature.

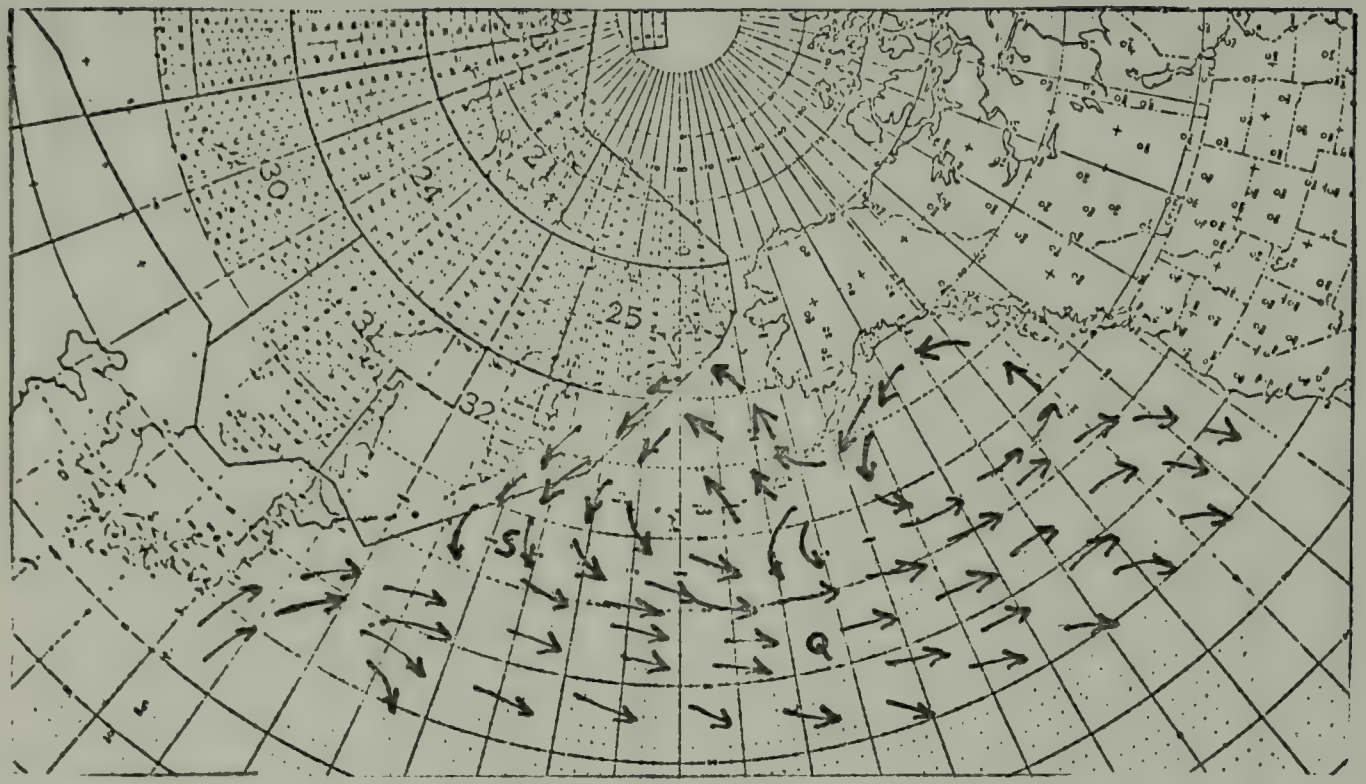

SCHEMATIC OF OCEAN CURRENT CIRCULATION IN THE VICINITY OF Q AND S

FIGURE 2

2. Exact start and stop times of weather phenomena as noted by the shipboard observer, and
3. RAOB's taken at 03Z and 15Z daily which consisted of temperature and humidity traces (wind's aloft information was not available).

To obtain sea surface temperature gradient magnitudes, mean sea surface temperature charts for the North Pacific were utilized [6]. Daily synoptic weather patterns were obtained from the U.S. Weather Bureau daily map series [19]. This series provides a daily 1230Z surface synoptic analysis of the Northern Hemisphere.

The preceding materials were the basis for data used in this study.

B. TREATMENT OF THE DATA

The microfilm format of the data dictated a manual analysis of the parameters being considered. In view of the quantity of material available, the consideration of the data was restricted to the months of May and June, 1953. Climatological reasoning was paramount in the selection since May represents a transition from the infrequent occurrence of fog at these stations during the winter months to the much more numerous fog occurrences of the summer months as typified by June. The demarcation from few fog occurrences to relatively numerous fog occurrences is evident at both stations. The year 1953 was selected due to the availability of the daily synoptic map series for that year.

In accordance with the Eulerian viewpoint, time series were plotted at each station employing some 401 individual observations spanning 1203 hours at Station Q and 495 observations spanning 1485 hours at Station S. Continuity was assumed between adjacent point plots for the purpose of analysis and changes between each three-hourly observation were assumed to be linear. Plotted parameters taken at three-hour intervals included:

1. Station air, dewpoint and sea surface temperatures in degrees celsius,
2. Visibility in nautical miles,
3. Wind direction to the nearest 22.5° and speed in knots,
4. Surface pressure in millibars,
5. Ceiling height in feet, and
6. Weather type and duration including exact start and end times.

In addition, temperature and relative humidity soundings were plotted at twelve-hour intervals. Figure 3 is an example of a typical time series plot of these quantities at Station Q. A continuous history of the changes in weather at the fixed stations with time is presented by this Figure.

The use of the time series charts coupled with the daily synoptic map series, and the mean sea surface temperature charts for the months of May and June as shown in Figures 4 and 5, enable the specific cases of fog occurrence at Ocean Stations Q and S to be analyzed in detail.

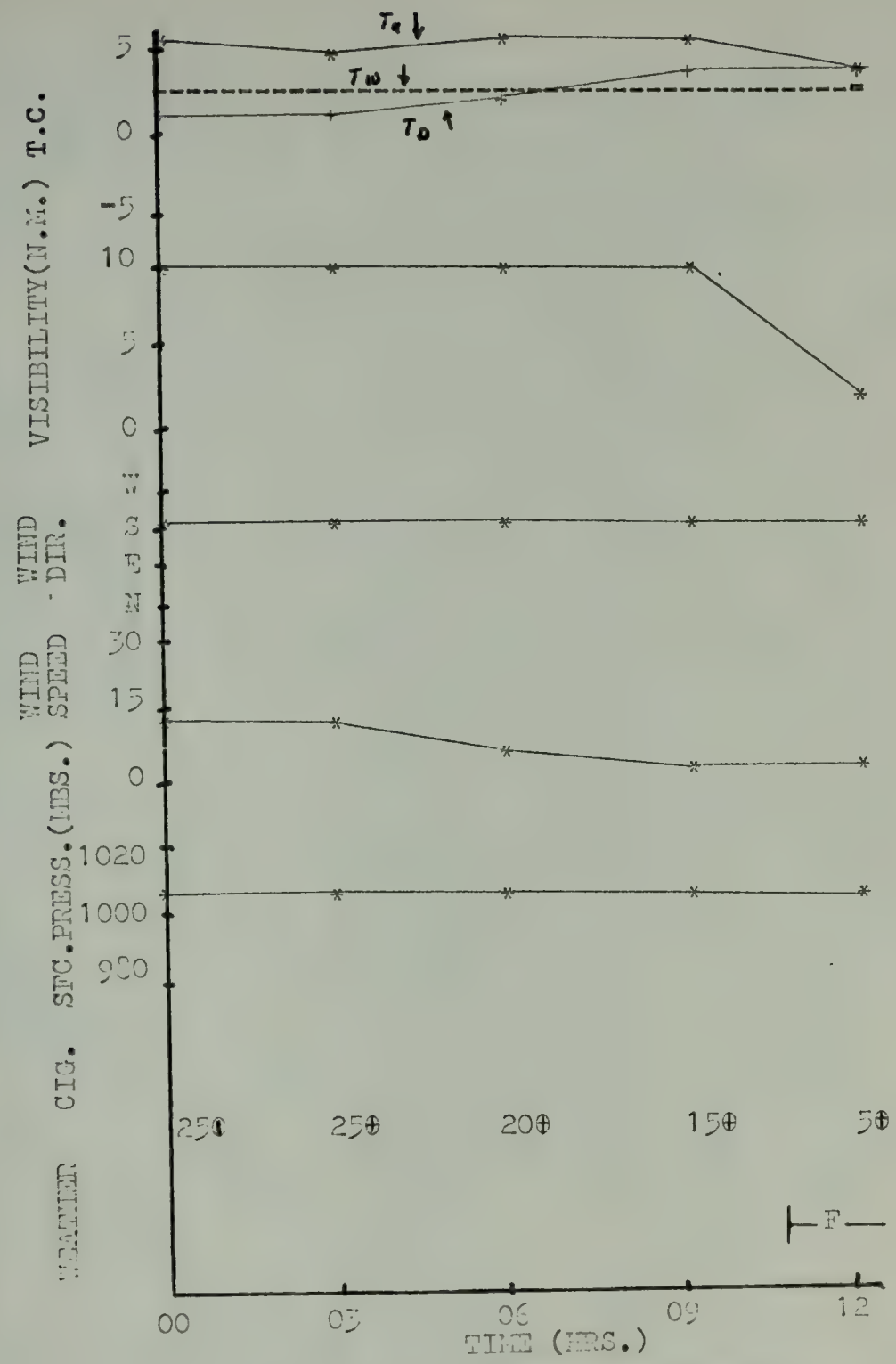

EXAMPLE OF TIME SERIES ANALYSIS
FIGURE 3

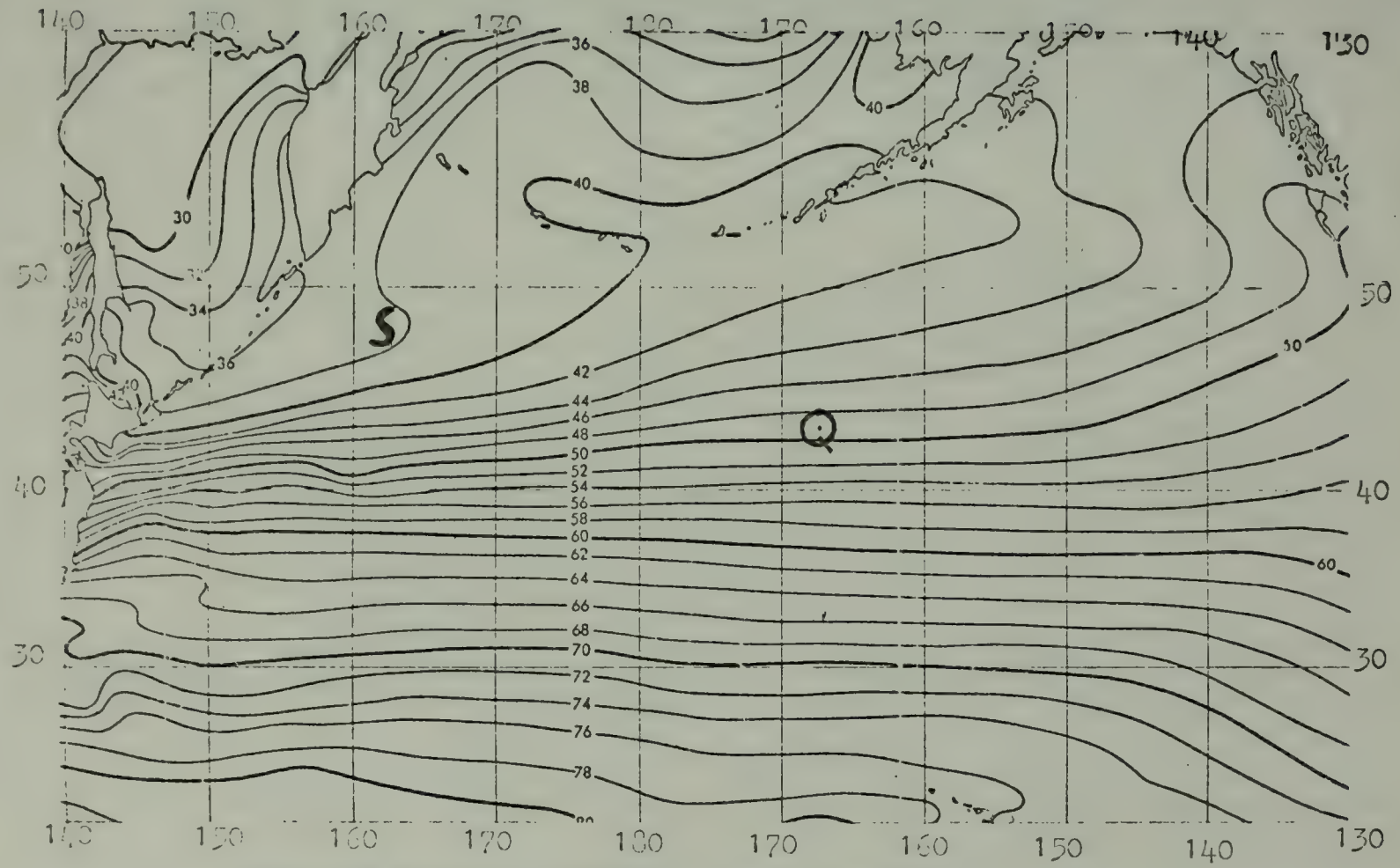

MEAN SEA SURFACE ISOTHERMS - MAY (After [6])

FIGURE 4

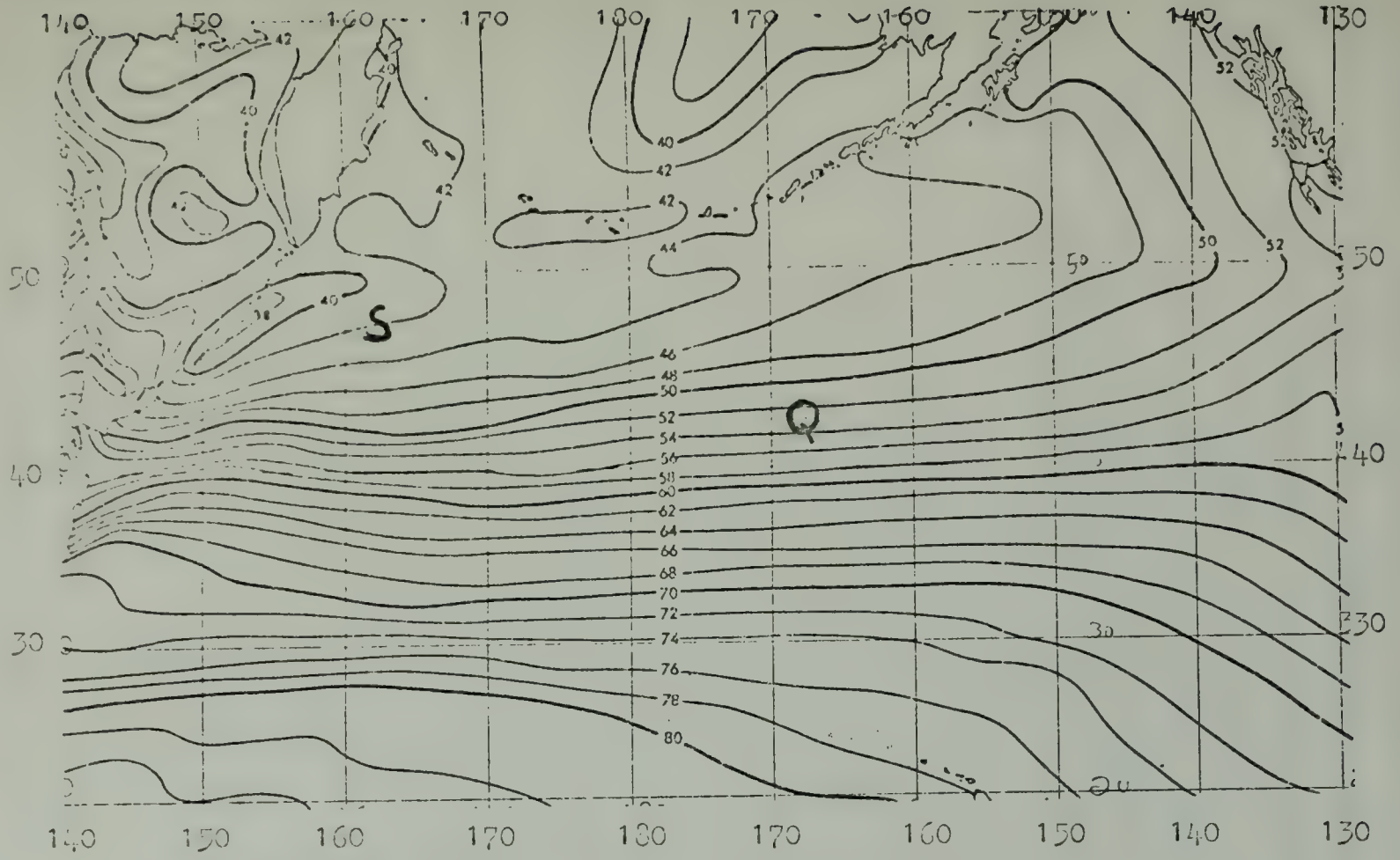

MEAN SEA SURFACE ISOTHERMS - JUNE (After[6])

FIGURE 5

In the following analysis, the term "fog" refers to the condition of restricted surface visibility due to suspended water droplets as determined by the shipboard observer. The beginning and ending times of the fog as logged by the observer were used to delineate each separate fog occurrence. Within each determined fog case, individual initial measured visibilities were investigated. In 81% of the fog cases studied, the minimum visibilities reported were less than 1/2 mile.

IV. ANALYSIS

In an effort to relate the change of the parameters mentioned in Chapter III to the occurrence of fog at Stations Quebec and Sierra, case studies of each fog occurrence during the months of interest were made at each station. These case studies consisted of two phases:

1. The analysis of the change in those quantities plotted on the time series, and
2. The synoptic conditions existing before, during and after each fog case.

The time series analysis was conducted with the aim of discovering the significance of each individual parameter upon the formation of the fog. This particular analysis was itself divided into two parts. The first of these was comprised of that group of parameters which applied to the surface meteorological conditions as measured at the ship. This group consisted of the air temperature, dewpoint, sea surface temperature, wind speed and direction, sea level pressure and visibility. Temperature rates of change were calculated from the time series for evaluation as to the effect of their magnitude upon the formation of the fog. Continuity between the observations was assumed and the values three hours prior to and after the central time were considered. The interval of the difference was, therefore, six hours. This central difference rate was performed for values of air

temperature, dewpoint, air temperature minus dewpoint, air temperature minus sea surface temperature and the dewpoint minus sea surface temperature. The resultant rates of change were compiled for periods of three, six, nine, twelve, fifteen, eighteen, twenty one, and twenty four hours prior to fog formation. Although the exact beginning and ending times of the fog were known, the three-hour interval between observations taken at the ship caused the selection of that observation taken closest to the fog beginning as the reference for the preceeding rate determinations.

It was thought that those parameters which had been analyzed in time series were the most obvious yardsticks by which the formation of the fog might be forecast, and indeed the air temperature minus the water temperature relationship was one of those investigated by Taylor [17]. Secondarily, these parameters are eminently available to shipboard meteorologists and as such were deemed to be useful parameters to employ in shipboard forecasting of fog.

The second part of the time series analysis consisted of investigating the change in the thermal structure and moisture content of the surface to 750 mb. layer of the atmosphere by considering the time sequence of pre-fog radiosonde soundings taken at each station. Various relations including the thickness of the inversion, the strength of the inversion, the maximum temperature of the sounding, in relation to the sea surface temperature, and the comparison of the sounding to an adiabatic profile were investigated.

The importance of the inversion strength to the duration of the resultant fog was of particular interest.

To make synoptic sense out of the Eulerian information obtained, it was necessary to examine the orientation of pressure systems surrounding the stations being analyzed. The purpose for this was three-fold.

First, it was of interest to determine the trajectories of the air crossing the stations being analyzed, and the resulting cooling exposure with regard to the sea surface temperature gradients. To this end, "wind fetches" were determined subjectively from the daily sea level weather map series [19]. The term "wind fetch" denotes the geometrical area over which winds of approximately uniform speed and direction are blowing. Resultant fetch dimensions were determined by combining pre-fog sea level pressure maps to obtain a mean flow area, and mean wind speed. Initial conconditions with regard to air temperature and dewpoint were obtained at the leading edge of the fetch from plotted ship reports as analyzed on the daily map series. The angle of crossing between the sea surface isotherms and the mean wind vector of the wind fetch was determined. This quantity was of interest in determining rates of cooling (if any) to which the air transiting the fetch was being subjected due to exposure to the sea surface temperature.

The rate of cooling for those cases where fetches could be delineated was determined by use of the Åmot-Mosby

formula [5] for computing near surface temperatures in its unintegrated form. The equation is as follows:

$$d(Ta-Tw)/_{dt} = V\cdot Tw - dta/_{dt}$$

Ta is air temperature, Tw is sea surface temperature, and V·Tw is the rate of change of sea surface temperature along the wind fetch.

It was shown empirically by Mosby in 1933 and Boyum in 1962 that the term $\frac{dTa}{dt}$ could be expressed as:

$$dTa/_{dt} = K(Tw-Ta) - C$$

K and C are constants determined empirically from observations and equal to 0.28 and 0.13 respectively. The form of the equation then used was:

$$d(Ta-Tw)/_{dt} = 0.13 + |\vec{V}|\,|\nabla Tw|\cos(\vec{V},\nabla Tw) - 0.23(Ta-Tw)$$

$|\vec{V}|$ is the mean fetch wind speed. $|\nabla Tw|$ is the magnitude of mean sea surface temperature gradient under the fetch, and $\cos(\vec{V}, \nabla Tw)$ is the cosine of the angle between the wind direction of the fetch and the orientation of the sea surface temperature gradient relative to north.

The integrated form of this last equation is used in the FNWC computer scheme for air temperature change over the sea surface. For the purposes of this investigation, however, it was determined that the relative magnitude of the term $\frac{d\ (Ta-Tw)}{dt}$ was of interest, hence the unintegrated form was used for simple cooling rate calculations. The sea

Table 1

SHIP Q

DIRECTIONAL SEA SURFACE TEMPERATURE DIFFERENCES

Month	Direc-tion	Band	Mean Range,C.	Mean Gradient
May	N-S	53°N-43°N	5.0-9.4	+4.4C/600nm
	N-S	43°N-33°N	9.4-18.9	+9.5C/600nm
June	N-S	53°N-43°N	6.95-11.7	+4.75C/600nm
	N-S	43°N-33°N	11.7-21.1	+9.4C/600nm

Table II

SHIP S

DIRECTIONAL SEA SURFACE TEMPERATURE DIFFERENCES

Month	Direc-tion	Band	Mean Range,C.	Mean Gradient
May	N-S	58°N-48°N	0.0-3.3	+ 3.3C/600nm
	N-S	48°N-38°N	3.3-14.4	+11.1C/600nm
	E-W	162°E-152°E	3.3-2.2	- 1.1C/400nm
	E-W	152°E-142°E	2.2-5.0	+ 2.8C/400nm
	NW-SE	52°N152°E-50°N155°E	0.0-2.2	+ 2.2C/300nm
	NW-SE	50°N155°E-48°N162°E	2.2-3.3	+ 1.1C/300nm
June	N-S	58°N-48°N	5.0-5.6	+ 0.6C/600nm
	N-S	48°N-38°N	5.6-16.7	+11.1C/600nm
	E-W	162°E-152°E	5.6-3.3	- 2.3C/400nm
	E-W	152°E-142°E	3.3-6.7	+ 3.4C/400nm
	NW-SE	52°N152°E-50°N155°E	4.4-5.6	+ 1.6C/300nm
	NW-SE	50°N155°E-48°N162°E	5.6-4.4	- 1.6C/300nm

surface temperature magnitudes for indicated latitude bands and directions from O.S.V.'s Q and S were obtained from the climatological mean charts of the North Pacific [6], and are summarized in Tables I and II.

An additional motive for the synoptic scale analysis was to investigate the relative increase in the number of fog occurrences at the two O.S.V.'s from May to June as shown in Table III.

Table III

OBSERVATIONAL STATISTICS

SHIP	MONTH	TOTAL OBS. HRS.	TOTAL FOG HRS.	%	NO. OF CASES
Q	May	738	48	6.5	6
Q	June	465	120.5	25.9	9
S	May	744	69.5	9.3	7
S	June	741	235.6	31.8	17

The variability of the occurrence of fog from May to June is obvious at each station and the relationship of this variability to the tracks of cyclonic disturbances was investigated through the use of the daily map series [19]. From this map series, storm tracks were constructed which could be compared to the climatological tracks as a means of investigating this variability.

The third synoptic analysis concerned the strength of the pressure systems causing the trajectories at Q and S.

The central pressures of the pressure systems were plotted on the storm tracks mentioned above, and the intensity of those centers was considered as well as the closeness of their approach to the stations in an effort to determine what relationship the intensity and extent of the systems had upon the occurrence of fog at Q and S.

The results of these analyses are discussed fully in Chapter V under the subdivisions of Point Parameters, Inversion Relations, and Synoptic Results.

V. RESULTS

A. POINT PARAMETERS

The point station time series analyses at O.S.V.'s Q and S were examined in detail and the results which follow are a summary of the analysis of the plotted parameters shown in Figure 3. The order of consideration of these parameters was based on the following reasoning. First, it is desirable in fog forecasting to know whether or not special emphasis should be put upon some particular time of the day when fog is most likely to occur. For this reason the diurnal variability of the fog cases was investigated.

Second, it is widely accepted that formation of fog itself is dependent to a major degree upon the saturation of the air at the location in question. For this reason the relationship between the station air temperature and dewpoint was investigated next. This investigation is an anchor point which has been used extensively for land based forecast studies. In the ocean though, the effect of the existence of a surface which is approximately isothermal when compared to the air above it, requires its consideration in relation to the air and dewpoint temperatures in the process of fog formation. These relations were therefore investigated as well.

Third, the effect of the station pressure as an indicator of the pressure regime existant during the fog, and the

relationship between station pressure tendency and the likelihood of fog occurrence were studied. These quantities are again utilized in land forecast studies of fog occurrence and were an element of Grisham and Renard's analysis of general fog occurrence in the North Pacific [4].

Fourth, the effect of the strength and direction of the surface winds on both the occurrence of fog and the initial visibilities in the fog at each of these ocean stations were examined to determine their applicability to an objective forecast scheme. Wind strength is regarded as a measure of the amount of turbulent mixing which may be acting to influence the formation or dissipation of fog and the direction of flow may be indicative of which wind quadrants the forecaster should concentrate upon in making a fog forecast.

Fifth, and lastly, the rates of change of those parameters above for which positive results were obtained, were investigated to determine the practibility of forecasting the occurrence of fog at a point station through the use of time series analysis. The time frame during which the local forecast effort should be concentrated to achieve maximum results is of principal interest to this analysis.

The investigation of diurnal variability in all fogs occurring at the two stations, both airmass cases and those cases involving precipitation, is displayed in Figures 6 (a) and 6 (b). The local onset time of the fog was plotted versus duration and frequency of occurrence respectively to determine if fog formation and resulting duration is

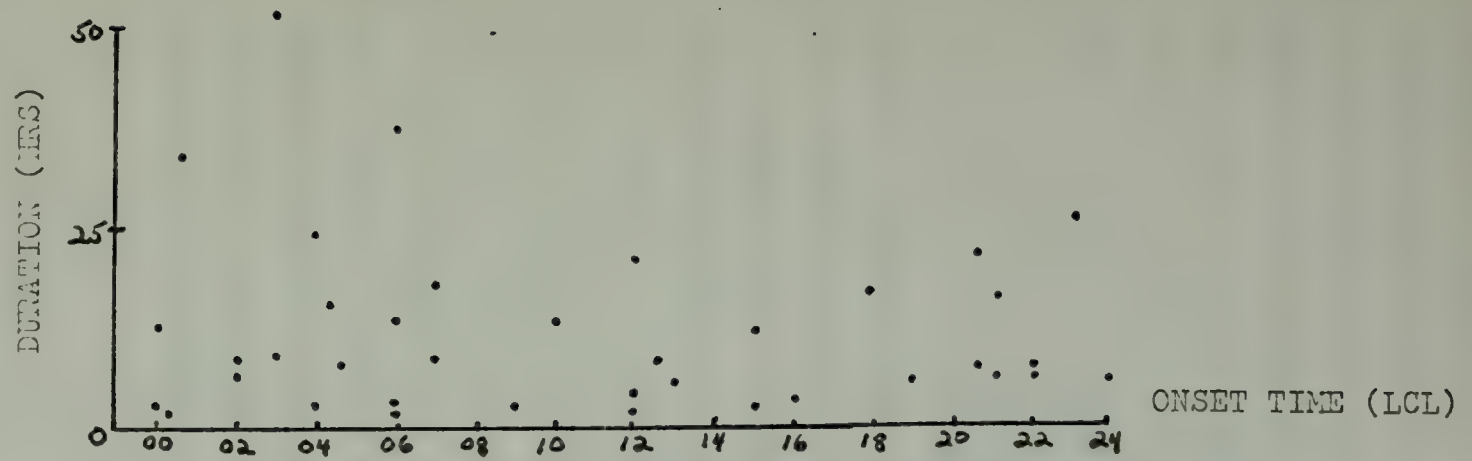

6(a) FOG DURATION VERSUS ONSET TIME - ALL FOG CASES

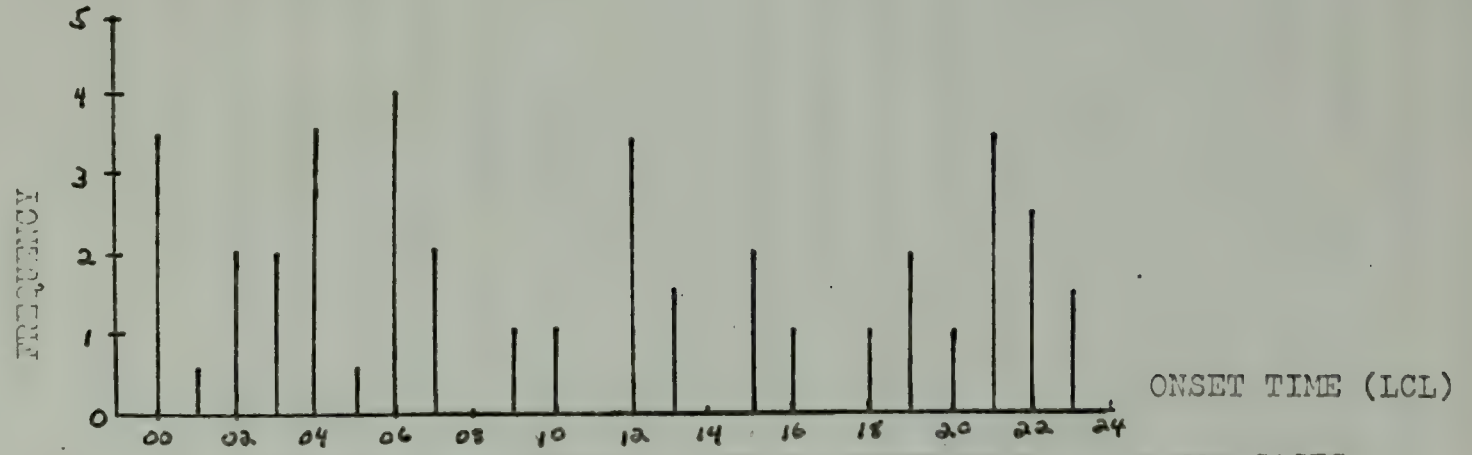

6(b) FREQUENCY OF OCCURRENCE VERSUS ONSET TIME - ALL FOG CASES

FIGURE 6 (a) - (b)

favored at some preferred local time. From the Figure 6 (b) it can be seen that no particular time of day is more favorable for fog formation than any other. 6 (a) reveals, however, a slight tendency for the long duration fogs to form in the early morning hours. A consideration of airmass only cases in the same manner in Figure 7 (a) and 7 (b) reveals that the long duration fog cases show a slight preference for an onset time in the late afternoon-early evening time span. Frequency of occurrence at any particular hour, however, seems to be fairly well distributed with no preference for a particular time of formation in either case.

Temperature relationships were examined to determine the ranges within which fog and no-fog occurrences fall. Figure 8 is a plot of the frequency of occurrence of fog and no-fog cases for specific ranges of air temperature (Ta) minus dewpoint (Td). The ranges are in half-degree increments with the upper boundary of the increment included in the range e.g. $0 \leq x \leq 0.5$. The difference was taken at 1000 LOCAL for the no-occurrence fog days, and at the fog onset time for fog cases. From this Figure it can be seen that no-fogs occurred for a (Ta-Td) difference greater than 2C., and that 85% of all fog cases occurred for a (Ta-Td) difference of 1C. or less. The occurrence of fog in the 1C. to 2C. range of (Ta-Td) was 15% of the total cases. The occurrence of fog with relative humidities less than 100% has been noted in the Arctic by Gathman and Larson [3] and possible explanations include instrument error and the existence in the fog of dry eddies in which no fog droplets exist. It

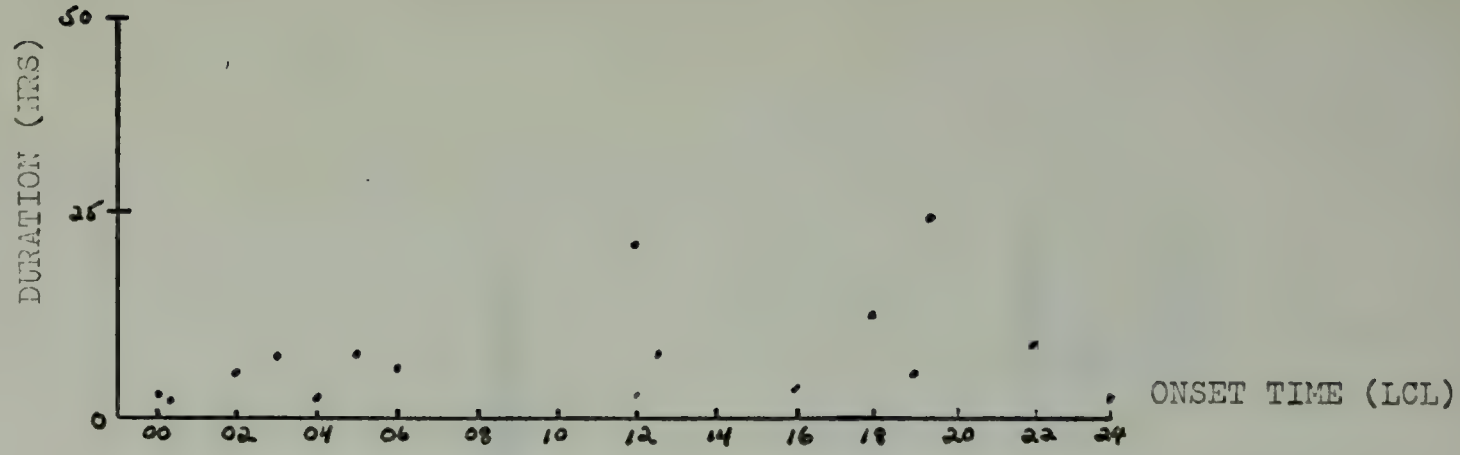

7 (a) FOG DURATION VERSUS ONSET TIME - AIRMASS ONLY

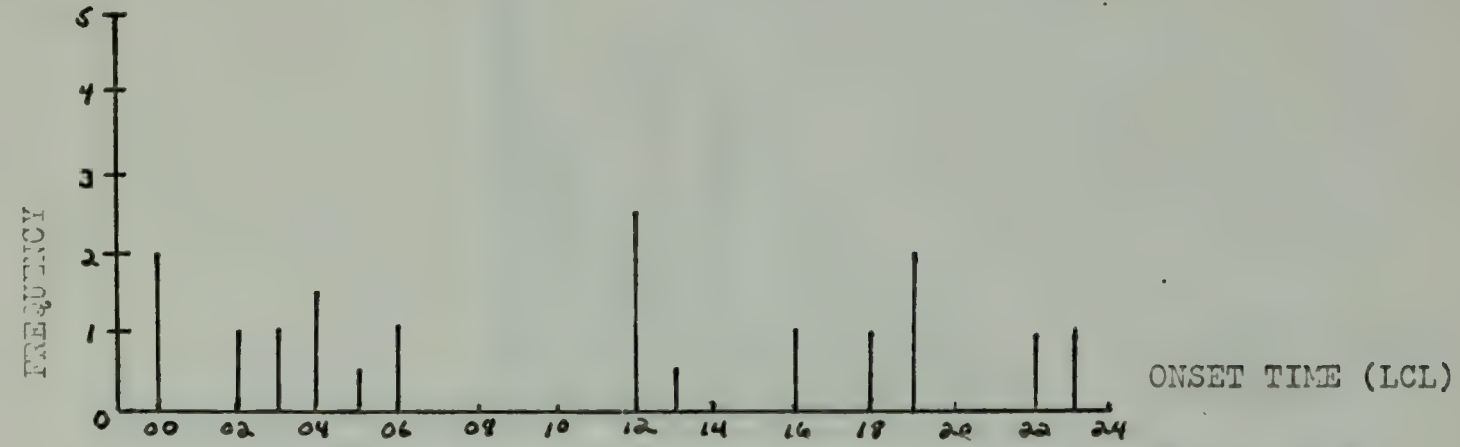

7 (b) FREQUENCY OF OCCURRENCE VERSUS ONSET TIME - AIRMASS ONLY

FIGURE 7 (a) + (b)

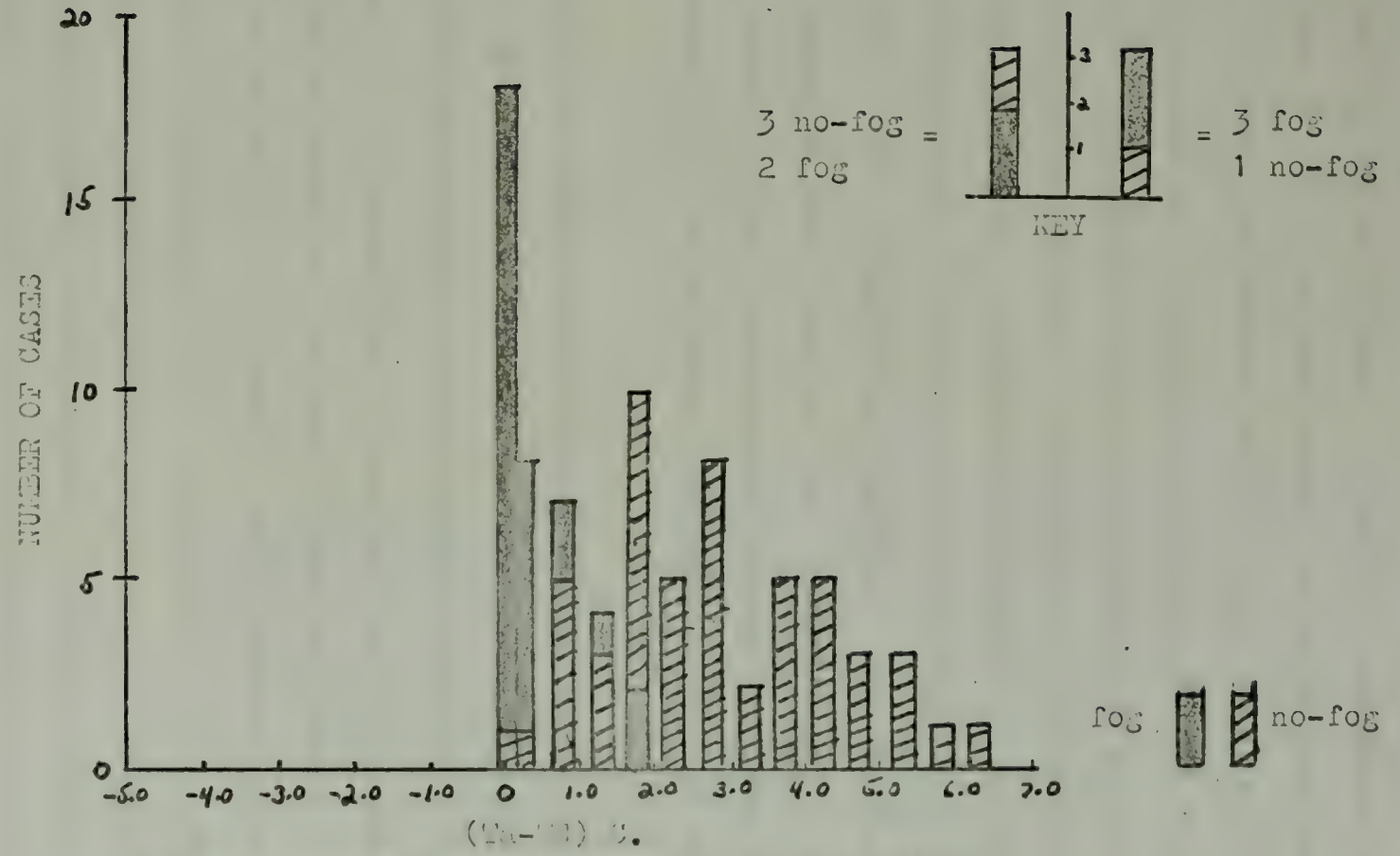

AIR TEMPERATURE MINUS DEWPOINT - ALL FOG CASES

FIGURE 8

appears most likely in the case of the Ocean Station Vessel that the method of measurement of the air temperature and dewpoint may be of prime importance. The main instrument used was a sling psychrometer and readings taken from this particular instrument are particularly susceptible to error if it is not aspirated at the correct speed, or the wet-bulb is improperly moistened. The effect of the existence of the ship itself as a perturbing influence on the temperatures measured from it is another consideration which might explain the (Ta-Td) separations observed. Data at the two O.S.V.'s examined here, however, were insufficient to determine the cause for the subsaturated readings in these fog cases, hence, conclusions about the separations are not possible.

Figure 9 is a plot of initial visibility corresponding to values of (Ta-Td) grouped in the ranges in Figure 8. It can be seen that the initial visibilities for those cases where the (Ta-Td) separation is greater than 0.5C. ranges from 0.25nm to seven nm, indicating that the degree of saturation reported at the station using standard measurements may not be relevant to the visibility at that station. For those cases where saturation was reported, however, 75% of these had initial visibilities of less than three nm. Additionally 74% of all fog cases had initial visibilities of less than three nm, suggesting an upper limit to an initial visibility forecast.

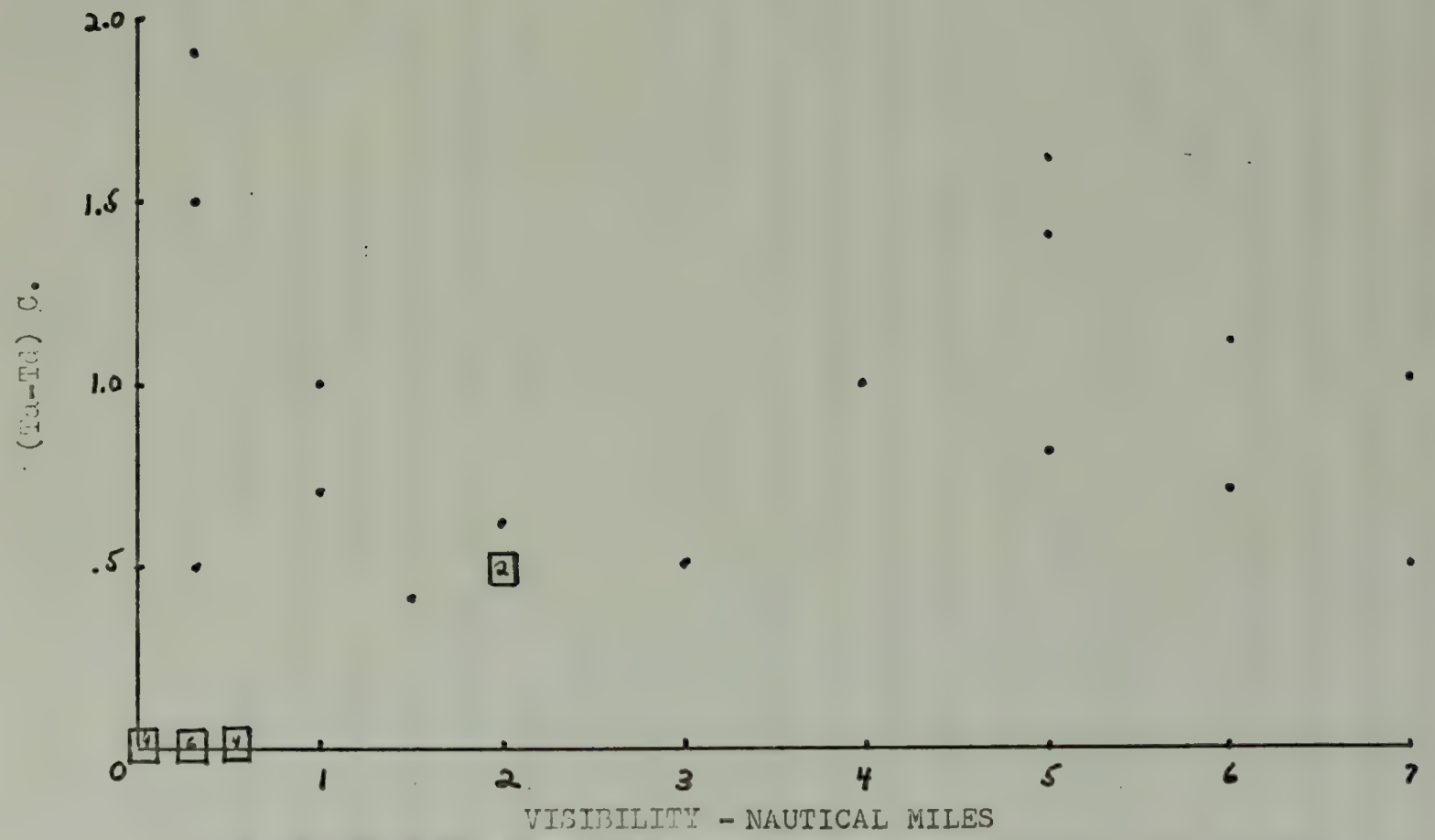

AIR TEMPERATURE MINUS DEWPOINT VERSUS INITIAL VISIBILITY IN FOG

FIGURE 9

It is evident from Figure 8 that fog occurrence becomes more and more likely as (Ta-Td) values drop below 2C., thus, this looks like a usable upper limit in fog forecasting. Further, for values of (Ta-Td) less than 0.5C. the ratio of fog to no-fog occurrences is 13:1. This means that for all cases where the (Ta-Td) difference was less than 0.5C. fog occurred 93% of the time.

The examination of the relationship of the local air temperature (Ta) to the sea surface temperature (Tw) led to Figure 10. The frequency of occurrence of specific ranges of values in 0.5C. increments of (Ta-Tw) were totaled. It can be seen that fog occurred with the air temperature from -2C. below the sea surface temperature to the air temperature of +5C. above the sea temperature. The majority of the fog occurred with the air temperature from 0 to 1.5C. above the water temperature. The no-fog cases show a similar distribution. The main indication from the Figure is that the air temperature at the stations is fairly conservative, remaining generally within $\pm$ 3.0C. of the sea surface temperature. The two fog cases indicated in the 3.5 to 4.0 and 4.5 to 5.0C. ranges seem to be related to strong local temperature rises and a combination of southerly flow and clearing at the Station Q. The mixture of fog and no-fog cases seems to preclude the use of air temperature in conjunction with sea temperature as a fog indicator in this sense, namely as a point measured difference. The dewpoint

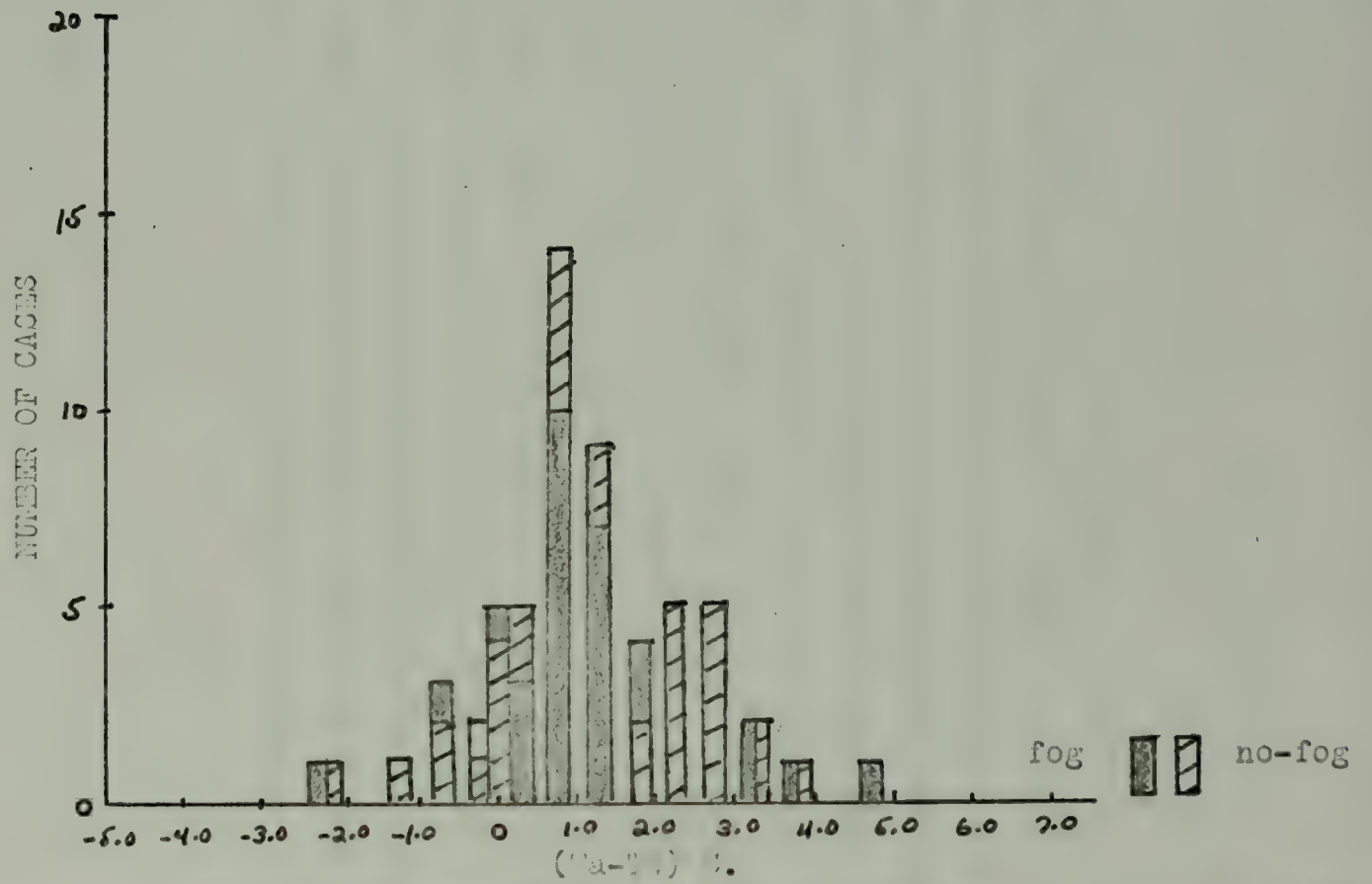

AIR TEMPERATURE MINUS SEA SURFACE TEMPERATURE - ALL FOG CASES

FIGURE 10

(Td) minus sea surface temperature (Tw), on the other hand, shows a better relationship between fog and no-fog occurrences.

Figure 11 is a plot of (Td-Tw) ranges versus numbers of occurrences of fog in each category. Again the 1000 LCL (Td-Tw) value was used for those days which exhibited no fog. Like the (Ta-Td) plot of Figure 8, Figure 11 shows a definite increase in fog occurrence, in this case when the dewpoint reads to within 1C. of the sea surface temperature. For (Td-Tw) less than -1C. no-fog cases clearly dominate, and no fog cases occur for values of (Td-Tw) less than -2.5C. As the values of (Td-Tw) become positive, the ratio of fog to no-fog occurrences becomes greater and only two no-fog cases occur for (Td-Tw) greater than +1.0C. In the -0.5 to +5C. range there is a 50% chance of fog, while for values of Td 1.0C. or greater above Tw, there is an 84% occurrence rate. It must be remembered at this point that the dewpoint value for the no-fog cases represents a 1000 LCL value only. Fluctuations in the dewpoint certainly occur during the balance of the day and therefore, this 84% occurrence rate is with regard to the 1000 LCL dewpoint value compared to the initial dewpoint at fog formation only. It is noteworthy in Figure 10 that the upper value of air temperature over sea temperature was 5C. The lower limit of the dewpoint shows much greater range than the air temperature. In Figure 10 it can be seen that the air temperature fell to a minimum of 2.5C. below the sea

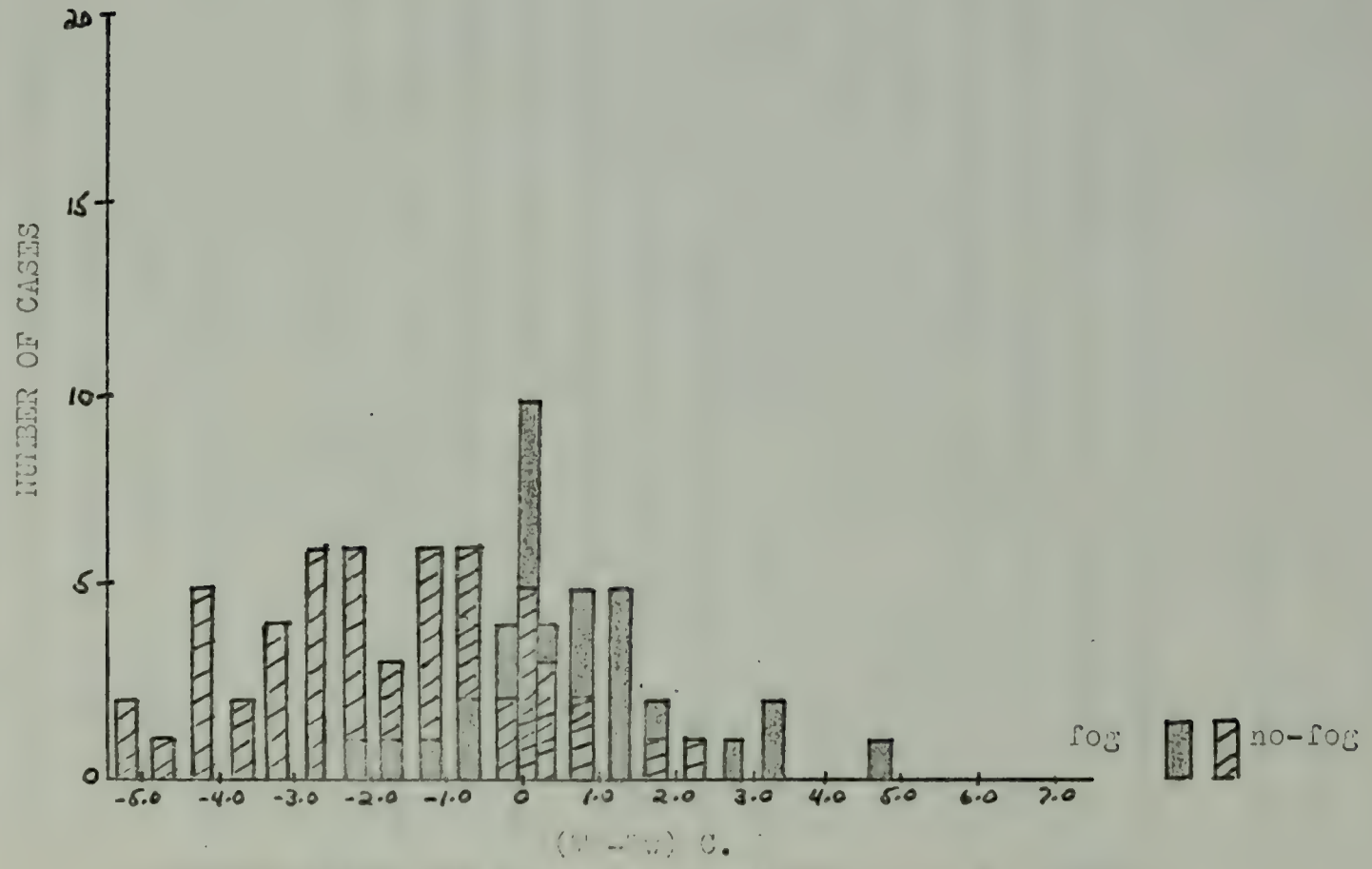

DEWPOINT MINUS SEA SURFACE TEMPERATURE - ALL FOG CASES

FIGURE 11

surface temperature. In Figure 11 the range of (Td-Tw) descends to -5.5C. indicating a greater variability in the dewpoint than the air temperature and, since the dewpoint is an indirect measure of it, in the moisture content of the air itself.

A comparison of initial visibility to the corresponding value of (Td-Tw) was made in Figure 12. No concrete relationships in the scatter which is presented are evident other than that the very low visibility cases are mainly concentrated in the 0 to +1.5C. range of (Td-Tw). Since high visibility fog cases also occur in the range no conclusion can be drawn about this relationship. It must be noted that the concentration of low visibility fogs in this range is probably a function of the fact that the majority of fog cases occurred with the air temperature minus water temperature value in this same range, and with an air temperature minus dewpoint temperature difference less than 2C. Again since the upper limit of the dewpoint is the air temperature, this clustering is to be expected in Figures 9 and 12.

In an effort to determine the station pressure relationship to the occurrence of fog at each station, Figure 13 was prepared. It was determined from the time series plots that diurnal pressure variations at the individual stations were of secondary importance, hence the 1000 LCL station pressure was selected as representative of no-fog occurrence

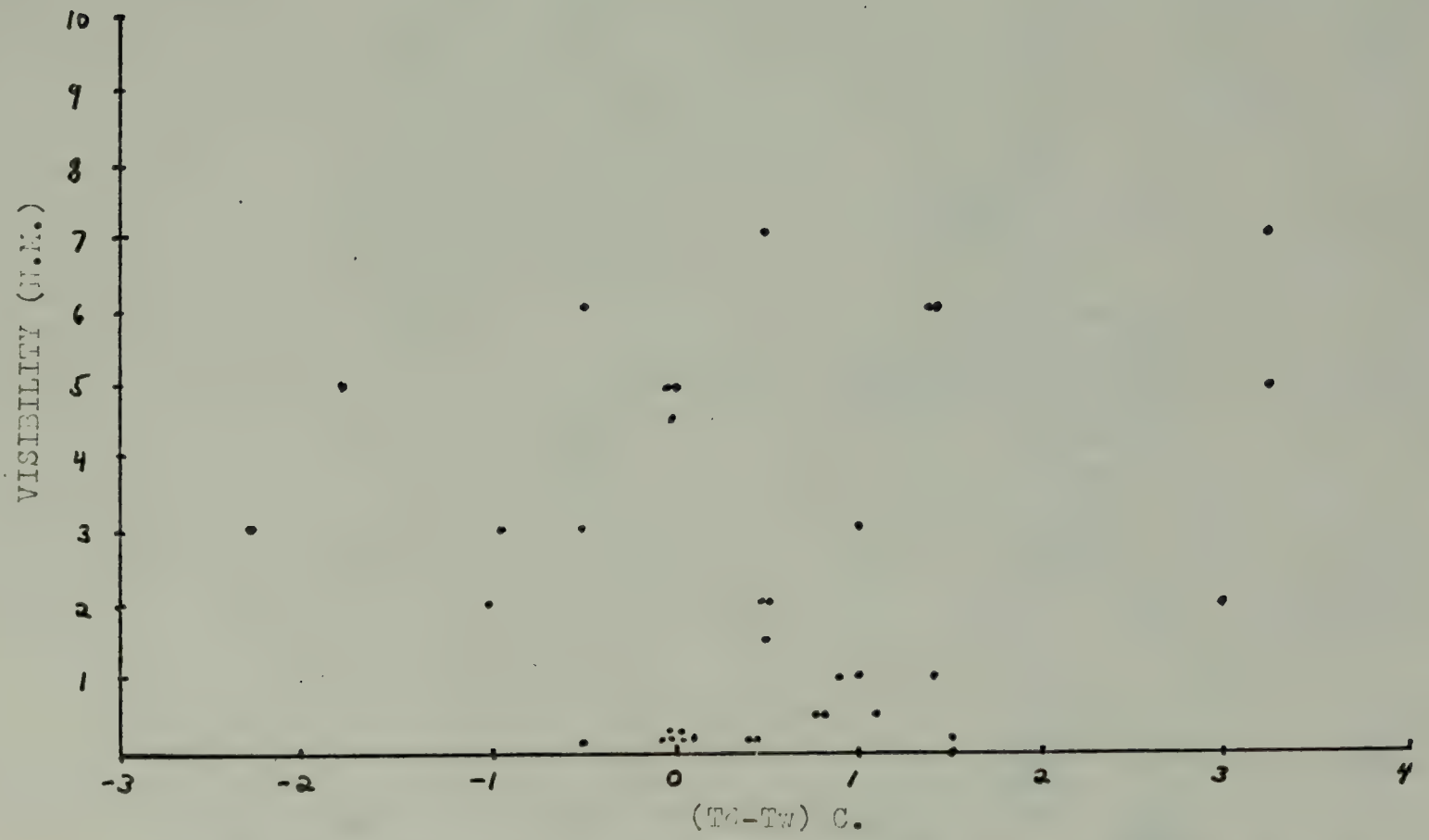

DEWPOINT MINUS SEA SURFACE TEMPERATURE VERSUS INITIAL VISIBILITY IN FOG

FIGURE 12

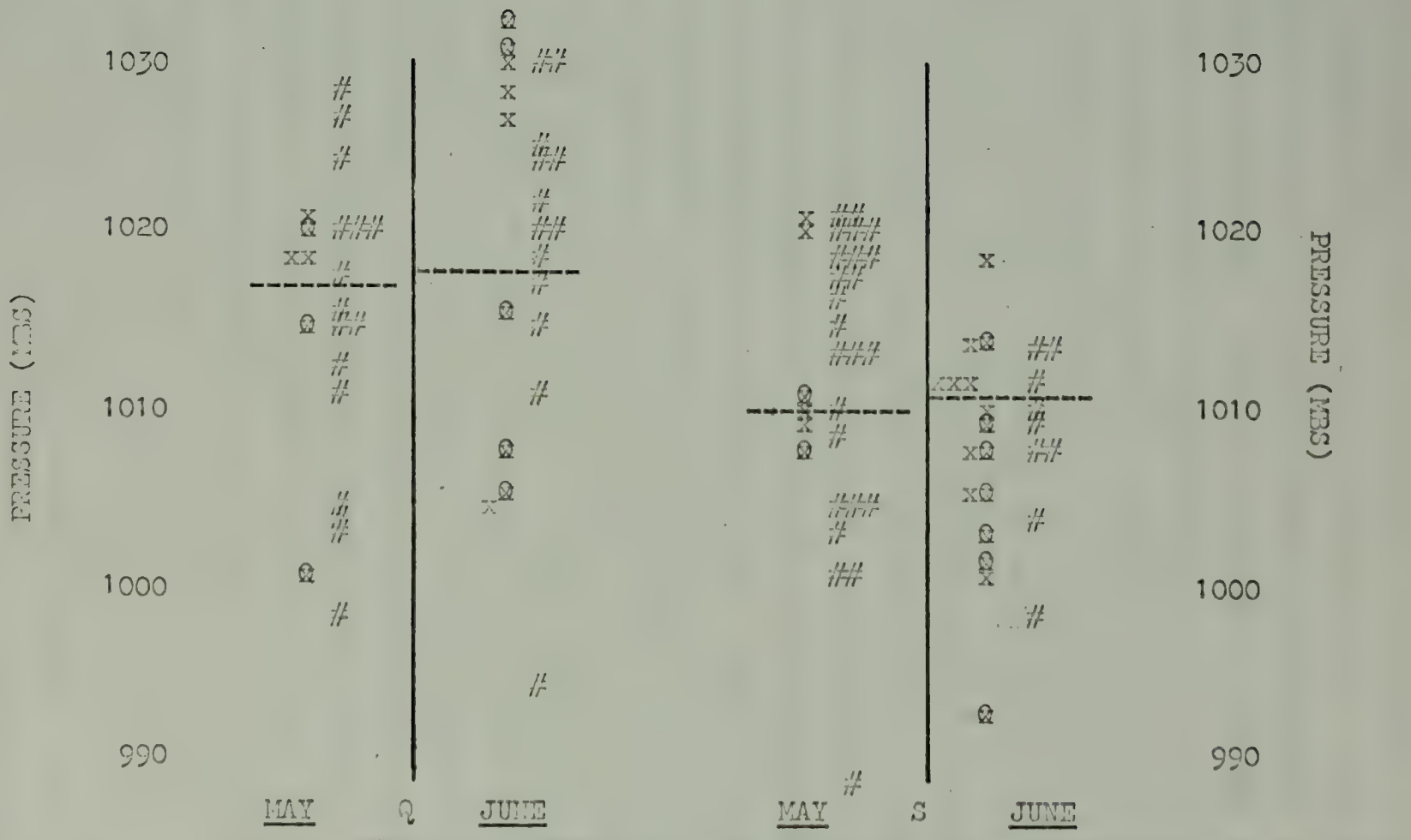

FOG AND NO-FOG PRESSURE DISTRIBUTION

FIGURE 13

days. The values for station pressure at the onset of each fog case were used for those days with fog. Figure 13 reveals that fog can occur throughout the pressure regime at each station. Climatological mean pressures are indicated for each station in each month, and it is noted that with the far more prevelant fog at each station in June, the mean pressures have risen one millibar from May to June at each station. It would appear at Station S, however, that the climatological mean is somewhat higher than the actual mean pressure for the month of June 1953. The actual mean for the plotted cases is 1008 mbs., some 4 mbs. lower than climatology. This may be of some significance when combined with the monthly storm tracks. Those cases of frontal fog indicated on the pressure plots span a rather wide range of values and this result was surprising. Frontal fog in this case consists of those fogs for which the dewpoint is caused to increase due to the effect of precipitation. It had been expected that the occurrence of frontal fog would take place in the lower half of the pressure regime with respect to the climatological means. Generally this is the case except for the two cases at Station Q during the month of June which occurred as precipitation developed in a high pressure domain as a warm front approached the station from the south. It follows, then, that though the frontal fogs will generally occur with lower pressure, they can also occur in high pressure domains given a frontal disturbance as a precipitation source.

Table IV is a summary of percentage of fog occurrences versus pressure tendency at each station and at both stations combined for all fog cases. A monthly breakdown for both stations is also provided. It is interesting to note that no fogs occurred at O.S.V. Q during rising pressure conditions indicating that at this station, frontal passage or high pressure center approach constitutes favorable conditions for no-fog during the months of May and June, 1953 at Q. S also shows no fog cases for rising pressure during the month of May. During June there is a 28.6% rate of occurrence for rising pressure as well as falling pressure. In every case the maximum percent occurrence is for steady pressure conditions. Steady pressure conditions infer either a stationary pressure pattern, or movement of the pressure systems in such a way that a constant isobar is maintained across the station. Either of these situations can be conducive to airmass fog formation if they result in moist air being advected and cooled over the station. Again, tracks of pressure centers will play a part in the determination of this latter question. Additionally, the examination of synoptic maps will resolve the determination of which fogs are airmass and which are frontal.

The effect of point winds upon the formation of fog at the O.S.V.'s is the subject of Tables V and VI, and of Figure 14. Table V summarizes those wind directions which existed at the onset of each fog case in percentage of the total cases. It is noteworthy that those wind directions

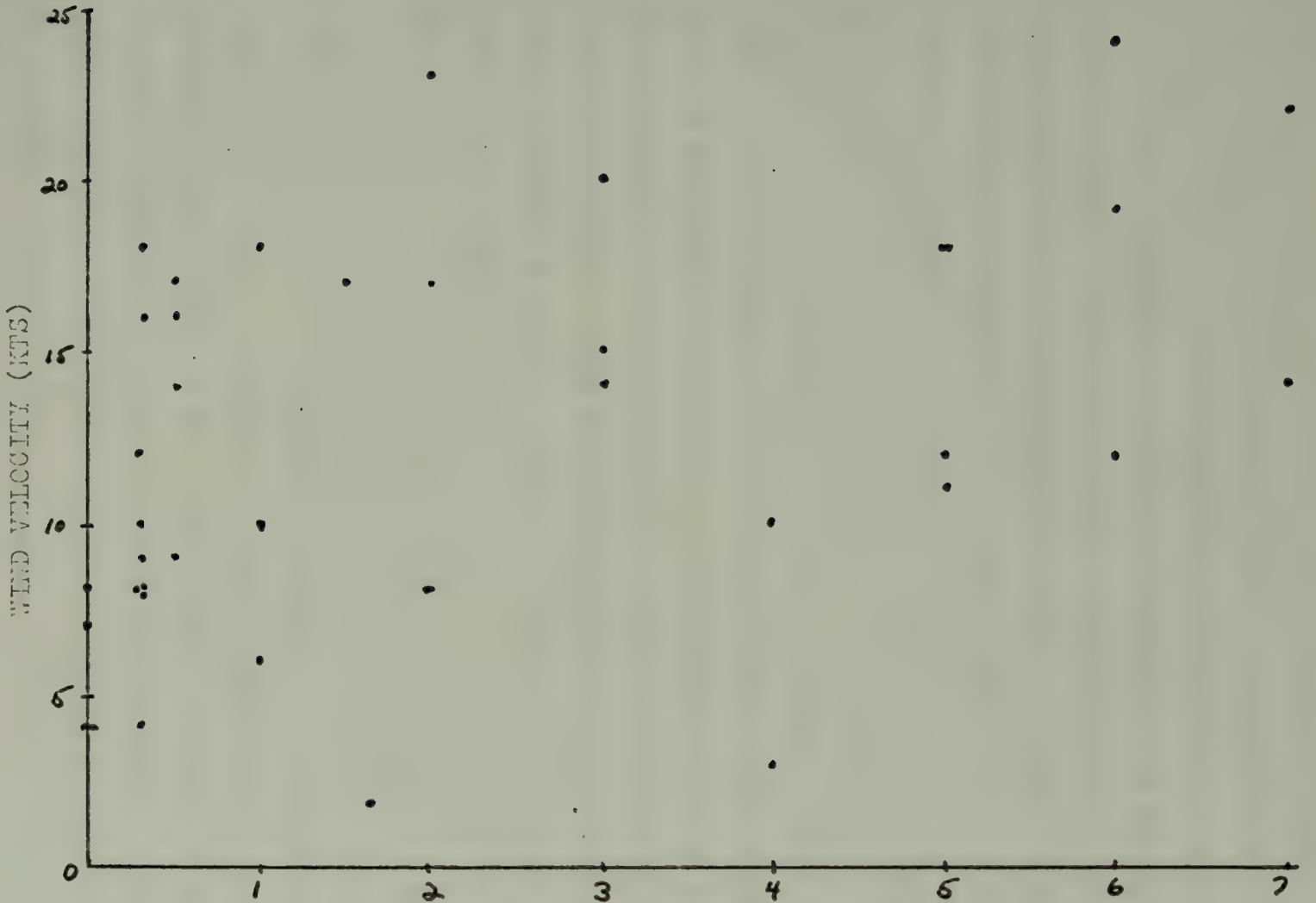

WIND VELOCITY VERSUS INITIAL VISIBILITY IN FOG

FIGURE 14

associated with fog at Q are predominately east through south west for both May and June, while Station S point winds show a fairly uniform distribution over direction, particularly for the month of June. It is evident that direction alone at the station cannot be used as a fog indicator. Rather, what must be considered is where the air came from. Table VI considers the velocity of the wind relative to fog occurrence for each station in both months under observation. An interesting result of these statistics shows that the very low wind speeds associated with land based fogs, particularly radiation fog, are absent in all cases save for the month of June at Station S where 20% of the cases fell into the lowest wind category. For the most part at Station Q, wind values of from 6 to 20 kts. account for 83.4% of the fog occurrence cases in May, and 80% in June. These statistics hold for the month of May at Station S as well, but the month of June shows the wider range which has been discussed. It is clear from this table that fog occurrence for winds greater than 25 kts. is extremely rare, with only 5% of the cases at S in the month of June falling into this category. No fog was reported for winds in excess of 30 kts. during these two months. Taylor [17] in his Grand Banks study did report fog with winds of up to 33 kts., so this suggests that an upward limit of 30 kts. for a cutoff velocity in making a fog forecast would be valid. In May and June at these stations it is noted that the occurrence of winds in excess

TABLE IV

PRESSURE TENDENCY-PERCENT OCCURRENCE

Pressure Rising	Pressure Steady	Pressure Falling
	All cases both ships	
14.6%	46.3%	39.1%
	Both ships May only	
-	40.0%	60.0%
	Both ships June only	
19.3%	48.4%	32.3%
	Q only May	
-	50.0%	50.0%
	Q only June	
-	66.6%	33.4%
	S only May	
-	50.0%	50.0%
	S only June	
28.6%	42.8%	28.6%

TABLE V

FOG OCCURRENCE PERCENT VERSUS SURFACE WIND OCTANT

Ship	Month	OCTANT							
		N	NE	E	SE	S	SW	W	NW
Q	May	-	-	33%	17%	17%	33%	-	-
	June	12%	-	12%	33%	12%	12%	-	19%
S	May	-	-	-	12.5%	25%	-	12.5%	50%
	June	10%	20%	-	15%	15%	10%	15%	15%

of 30 kts. occurred at Station Q for only 3.6% of the hours observed, and for 4.8% of the time at Station S. The generalization of this result cannot, therefore, be applied to other months and other areas of the North Pacific without further analysis.

The relationship of initial visibility during fog onset to the wind velocity is summarized in Figure 14. Although there is a great deal of scatter, it can be seen that the higher the wind speed, the greater is the likelihood of a high onset visibility, that is, one greater than one nautical mile. It is apparent that a fair number of cases of onset visibilities less than one nautical mile occur for wind speeds of from 10 to 20 kts., however as the wind speed climbs over 10 kts. the incidence of greater visibility increases as well. In a forecasting scheme wind speed would therefore be considered as a limiting value both to the occurrence and onset visibility of the fog itself at these stations.

The final analysis of the point time series concerned the rates of change of the temperature parameters prior to the formation of fog. The analysis technique described in Chapter IV was used to determine the rates of change of the air temperature and dewpoint temperature individually, as well as the difference between these two quantities themselves. In addition, the air-sea surface temperature and dewpoint-sea surface temperature differences were analyzed. The results appear in Table VII.

TABLE VI

FOG OCCURRENCE PERCENT VERSUS WIND SPEED

Ship	Month	Wind Speed Ranges					
		0 - 5	6 - 10	11-15	16-20	21-25	25-30
Q	May	-	16.6%	33.4%	33.4%	16.6%	-
	June	-	40.0%	-	40.0%	20.0%	-
S	May	-	25.0%	12.5%	50.0%	12.5%	-
	June	20.0%	30.0%	25.0%	10.0%	10.0%	5.0%

TABLE VII

RATES OF CHANGE
GREATEST TOTAL ACTIVITY (PERCENT OF ALL CASES)

d(Ta)/dt	d(Td)/dt	d(Ta-Tw)/dt	d(Td-Tw)/dt
35.0%	61.3%	3.4%	-

CENTRAL HOUR OF GREATEST RATE CHANGE PRIOR TO FOG FORMATION
PERCENT OCCURRENCE - ALL FOGS

	3	6	9	12	15	18	21	24 HR
Ta	29.6%	7.4%	26.0%	11.1%	14.8%	11.1%	-	-
Td	48.3%	13.8%	10.3%	3.4%	13.8%	6.8%	3.4%	-
(Ta-Td)	53.6%	10.7%	7.1%	7.1%	7.1%	7.1%	7.1%	-
(Ta-Tw)	34.6%	15.3%	7.7%	15.3%	7.7%	-	15.3%	3.8%
(Td-Tw)	35.7%	-	17.8%	3.5%	21.4%	10.7%	10.7%	-

From the upper line of Table VII, it is apparent that the dewpoint undergoes the greatest total activity for the majority of fog cases studied and that the air temperature accounts for the highest level of activity in approximately one third of the cases studied. The breakdown of hour of greatest change prior to the onset of fog reveals that each parameter undergoes its greatest change in the six hours prior to fog formation. This means that rate changes are probably not useful for "long term" (greater than nine hours prior to fog onset) forecasting. It appears from this table, however, that the dewpoint is a very key element in any prediction scheme for ocean fog, and based upon the percent of the cases where the dewpoint is more active, it seems to be more important than the air temperature. Noting the greater ranges in (Td-Tw) versus (Ta-Tw) in Figures 11 and 10 respectively may serve to explain this fact. It seems that the air temperature is controlled rather more by the sea surface temperature than is the dewpoint. Roll [14] points out that for warm air moving over a cold sea surface, if the dewpoint is higher than the sea surface temperature, moisture is lost to the sea surface temperature at approximately the same rate as the air temperature is cooled. It can be seen from Figure 10 that most no-fog cases occur for the dewpoint lower than the sea surface temperature. Figure 11 reveals that most fogs occur with the temperature of the air above the sea surface temperature. It follows then that the dewpoint must climb up to

the sea surface temperature, at least for fog formation to be likely.

B. INVERSION RELATIONS

The examination of the surface to 750 mb. level radiosonde soundings taken at each O.S.V. was considered important to the analysis of fog occurrence at each of these stations, as the existence of an inversion in connection with the occurrence of non-steam fogs is regarded as essential.

From sequential plots of the soundings taken prior to, during, and after each fog, specific profiles were taken which were representative of the types of fog which occurred at each station. There are three distinct types of profiles, each tied to a specific type of fog.

The first profile series is shown in Figure 15. This group of soundings is typical of those cases analyzed for which well defined southerly fetches could be determined. It was taken over the time frame of 17 June 1953 at 1500Z to 1500Z on 20 June 1953 at O.S.V. Q. At 1200Z on 18 June a warm front has passed the station and the resulting soundings are typical of those found in the warm sector of the cyclone system. Frontal precipitation is falling intermittenly during the sequence, but the main factor causing the inversion in this group of cases is low level warm air advection. The local sea surface temperature denoted by an "X" on the sounding serves as an anchor point, and the vertical dashed line on each sounding represents the upwards

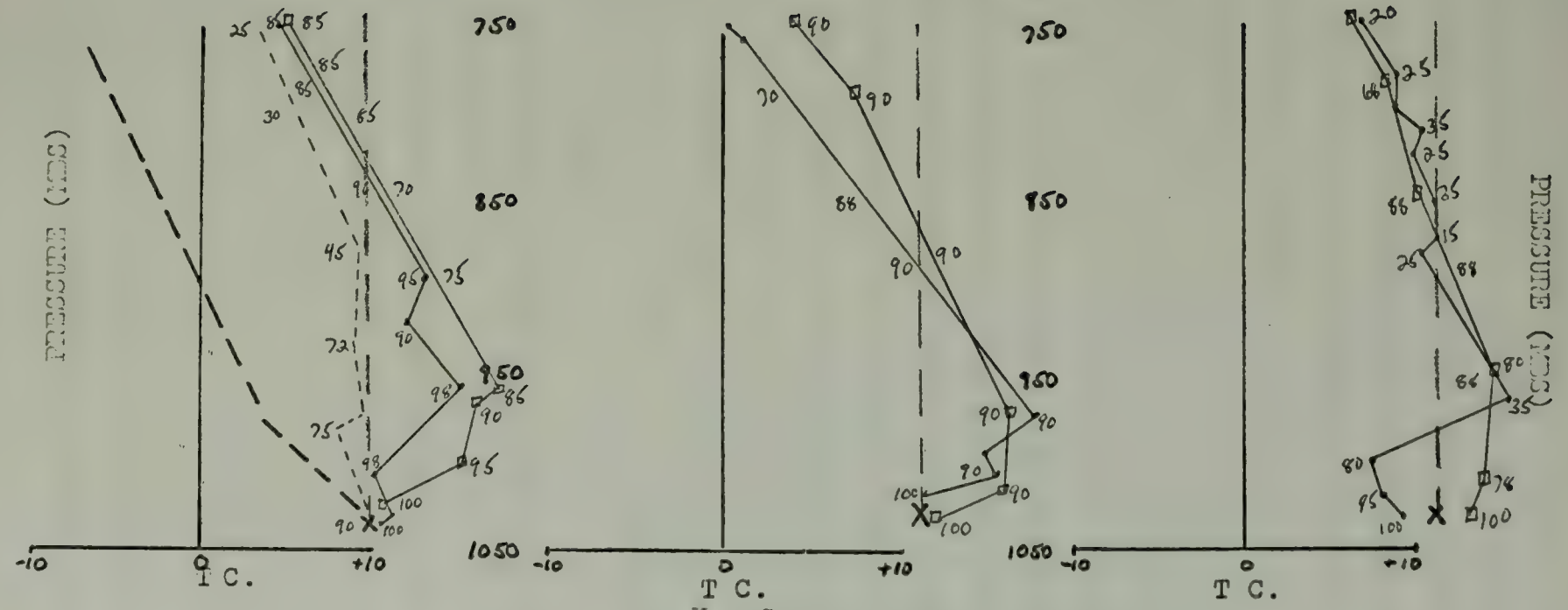

X = Sea Surface Temperature

= 17/15z
= 18/03z
= 18/15z
= 19/03z
= 19/15z
= 20/03z
= 20/15z

TYPICAL INVERSION SERIES FOR AIRMASS FOGS WITH ASSOCIATED PRECIPITATION

FIGURE 15

extension of the sea surface temperature. The area of the subsequent sounding to the right of this line is a measure of the degree and strength of the advection taking place. The cooling effect which the sea surface temperature exerts on the warm air from the south is evident in the formation of the surface to 960 mb. level inversion. The magnitude of the advection could not be estimated since intermediate 850 and 700 mb. charts were not available, however, the heavy dashed line on the sequence represents a typical adiabatic reference sounding. This reference is based on a surface temperature of 15C. and humidity of 85%. The sounding is dry adiabatic up to the lifting condensation level represented for the assumed temperature and humidity conditions, and moist adiabatic above the level. It can be seen that the lapse rates above the inversion parallel the moist adiabatic rate very well. The progression of this time series shows that the following sequence occurs for advection fogs:

1. Warm advection begins to show up in the prefog sounding,
2. The inversion is established and the warm advection continues, coupled with moisture advection in the surface to 750 mb. layer and precipitation, and
3. Saturation results at the surface and in the adjunct boundary layer.

A fourth possibility is shown in this particular sequence (Figure 15) but may or may not occur regularly. In the

20/15Z sounding it will be noted that drying aloft has occurred with subsequent clearing of the ceiling, enabling the fog layer to cool below the sea surface temperature. Since no cold air is being advected at this time nor subsidence effects being observed, based on analyses of the pressure systems, radiative cooling is the only factor which can account for this phenomena. This particular sequence was observed for 38% of the fogs occurring at O.S.V.'s Q and S during May and June of 1953. The effects of subsidence, or the sinking and adiabatic warming of air from aloft near the centers of high pressure areas were not observed to any great extent in the formation of these particular inversion sequences. Subsidence may, however, be an important mechanism in the formation or enhancement of inversions associated with fogs in other months at these stations.

Figure 16 shows the sequence of the occurrence of the second basic set of profiles for fog connected soundings. The basic profile appears quite similar to the profiles shown in Figure 15 with the difference that no precipitation is occurring during this fog. Additionally, no surface inversion is evident unlike the previous series in Figure 15. It must be noted that until 9 June at 1500 Z the air is warmer than the sea surface, hence, a shallow surface inversion must be present. The profiles as a group are much less humid aloft than the group in Figure 15 which involved precipitation falling. This is to be expected. It is also noticeable in Figure 16 that the falling of the surface air temperature below the sea temperature has again occurred.

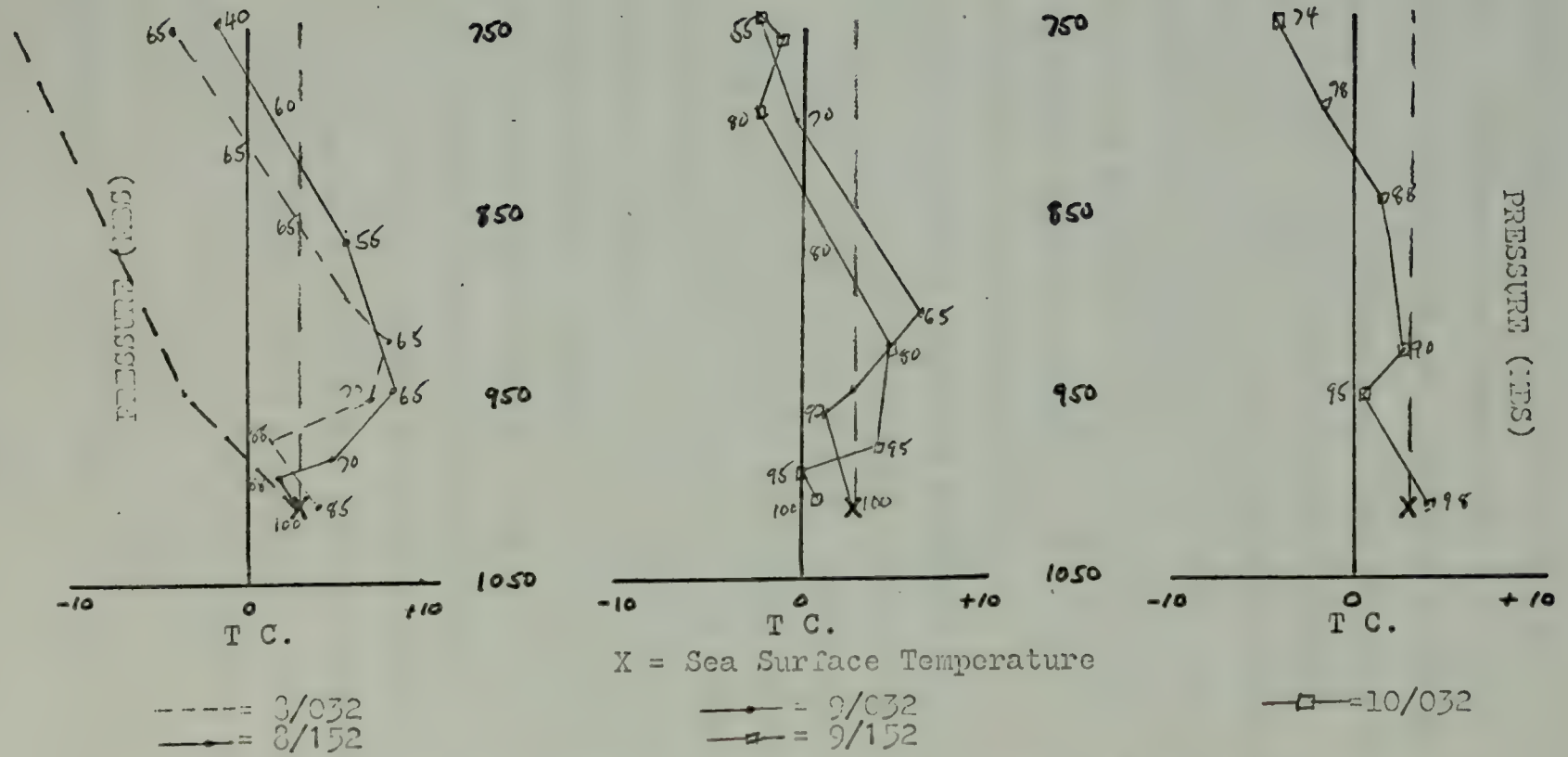

X = Sea Surface Temperature

3/032
8/152
9/032
9/152
10/032

TYPICAL INVERSION SERIES FOR AIRMASS FOGS WITH NO PRECIPITATION

FIGURE 16

Radiation must again be aiding in the maintenance and thickening of the fog. This particular sequence was taken at Station S on June 8-10, 1953. Again advection aloft has been occurring. However, the flow across S at this time is from the Northwest off the warmer Kamchatka Peninsula. It is, then, warm dry continental air being modified by the ocean to form fog at S which this inversion depicts. This profile series is similar to those attained by Leipper [8] in coastal fog studies, leading to the conclusion that land effects in the Northwestern North Pacific are important. This particular profile series was observed for 15% of the fogs occurring at Station S only.

The third group of specific profiles involved with fog occurrence is shown by Figure 17. The actual fog occurrence for this profile series is at 1900Z on 5 June, four hours after the center profile of Figure 17. This profile is distinctive in that it approaches the moist adiabatic lapse rate for its entire length up to the 750 mb. level. This particular type of profile was observed in 10% of the total fog cases studied at each station, and is associated with precipitation and thick stratus. The precipitation, in the form of moderate drizzle, causes a rise in the moisture content of the surface air and results in fog. This situation results from flow on the lee side of a stationary low to the east, and the sounding appears to be typical of the airmass one would expect in this situation. Eventually weak drying eliminates the fog, as shown in

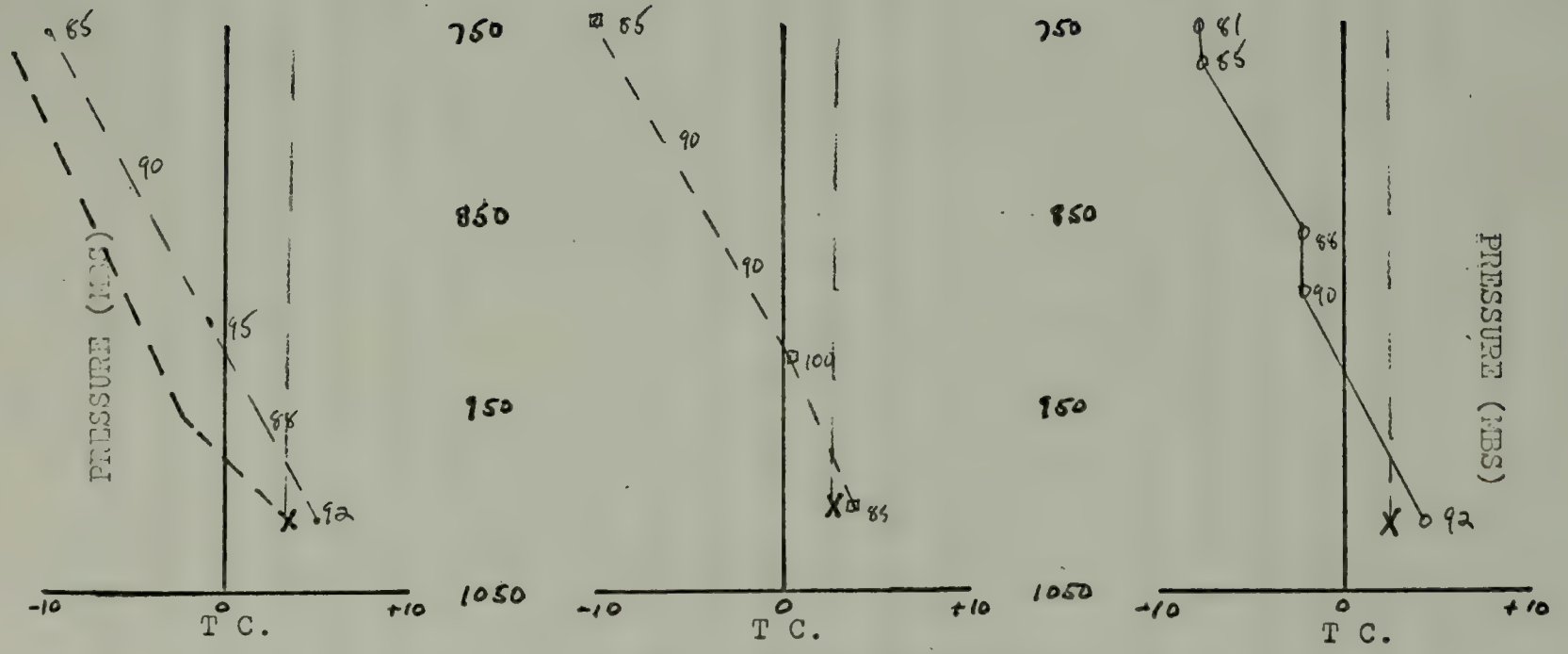

X = Sea Surface Temperature

----= 5/032 ---= 5/152 —o— = 6/032

TYPICAL INVERSION SERIES FOR FRONTAL FOGS WITH ASSOCIATED PRECIPITATION

FIGURE 17

the 6 June 0300Z trace in Figure 17 as the cold air advection makes itself felt.

These three basic profile groups represent the generalized traces at each O.S.V. for each case where fog occurred during May and June of 1953. A typical no-fog sounding is shown by Figure 18. What is most noticeable about this profile is that the lapse rates more closely approach the dry adiabatic lapse rate than did the profiles of Figure 17. Additionally, the relative humidities of the near surface layer are in the 80 to 88% range indicating relatively drier air moving across the station.

An examination of the effect that the inversion itself had upon the duration of the related fog was conducted for those cases where inversions with bases lower than 1000 ft. could be determined. It must be mentioned that those cases such as in Figure 17 where low level inversions were not evident were not included in this particular investigation even though the existence of the inversion could be inferred from the fact that the air was warmer than the sea surface. The reason for this is that no valid estimate could be made as to the thickness of the inversion in these cases.

Figure 19 shows the relationship between the thickness of the inversion and the duration of the related fog. The general trend from this Figure is that the thicker the inversion, the longer the duration of the resulting fog. It can be generalized from this that in areas of forecast warm air advection over cold surfaces it can be expected that

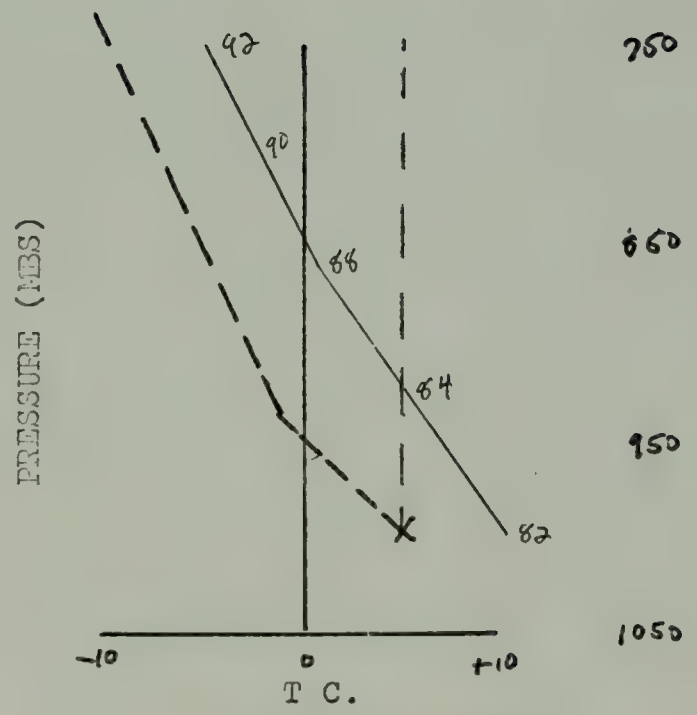

X = Sea Surface Temperature

TYPICAL NO-FOG SOUNDING

FIGURE 18

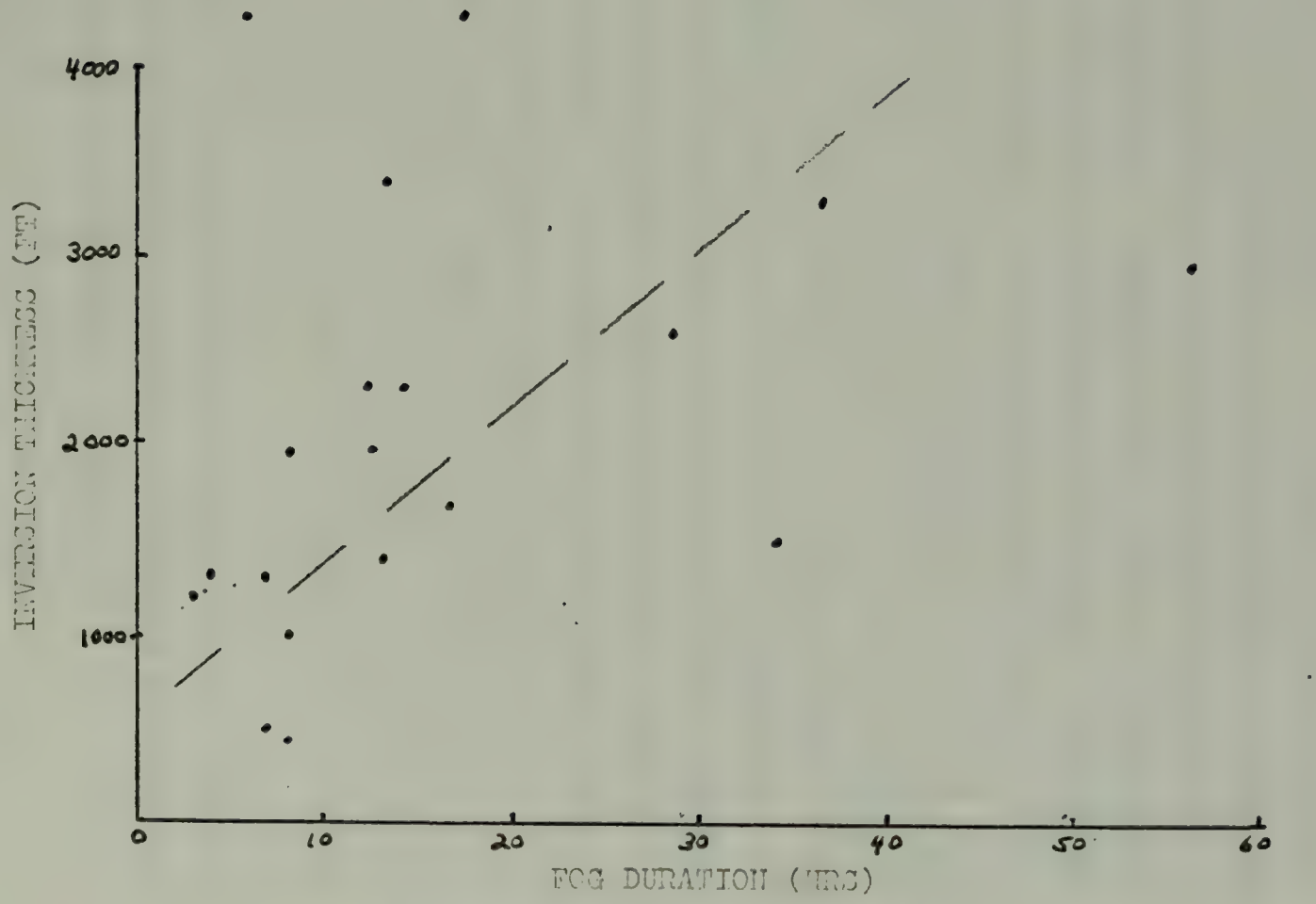

FOG DURATION VERSUS INVERSION THICKNESS FOR ALL FOGS WITH INVERSION BASES <1000 FEET

FIGURE 19

inversions will form. Once the inversion forms, if continued advection, or radiation from the resultant fog occurs, the inversion will thicken and the fog persist.

In an effort to determine how the strength of the inversion is related to the duration of the resultant fog Figure 20 was constructed. The value of the maximum temperature of the inversion minus the sea surface temperature as a quantity related to inversion strength was plotted versus fog duration. Again, a weak trend of long duration for large temperature differences was evident. When the average lapse rates of the inversions were calculated and plotted in Figure 21, however, the dependence was not apparent. This is rather interesting since it appears that the duration of the fog is related to the positive departure of the temperature aloft from the sea surface temperature as utilized in [7], yet the lapse rates, which are measures of the sharpness of the inversion have little relation to the resultant fog. An explanation of this might be that the quantity (Tmi-Tsst) measures how much advection has taken place and the greater the warm air advection aloft, the greater the amount of time required to mix down to the surface to break the inversion, and therefore, the longer it takes to lift the fog.

Figures 22 through 25 break Figures 20 and 21 into the two respective stations and each sub-grouping confirms the observations of the first pair of graphs.

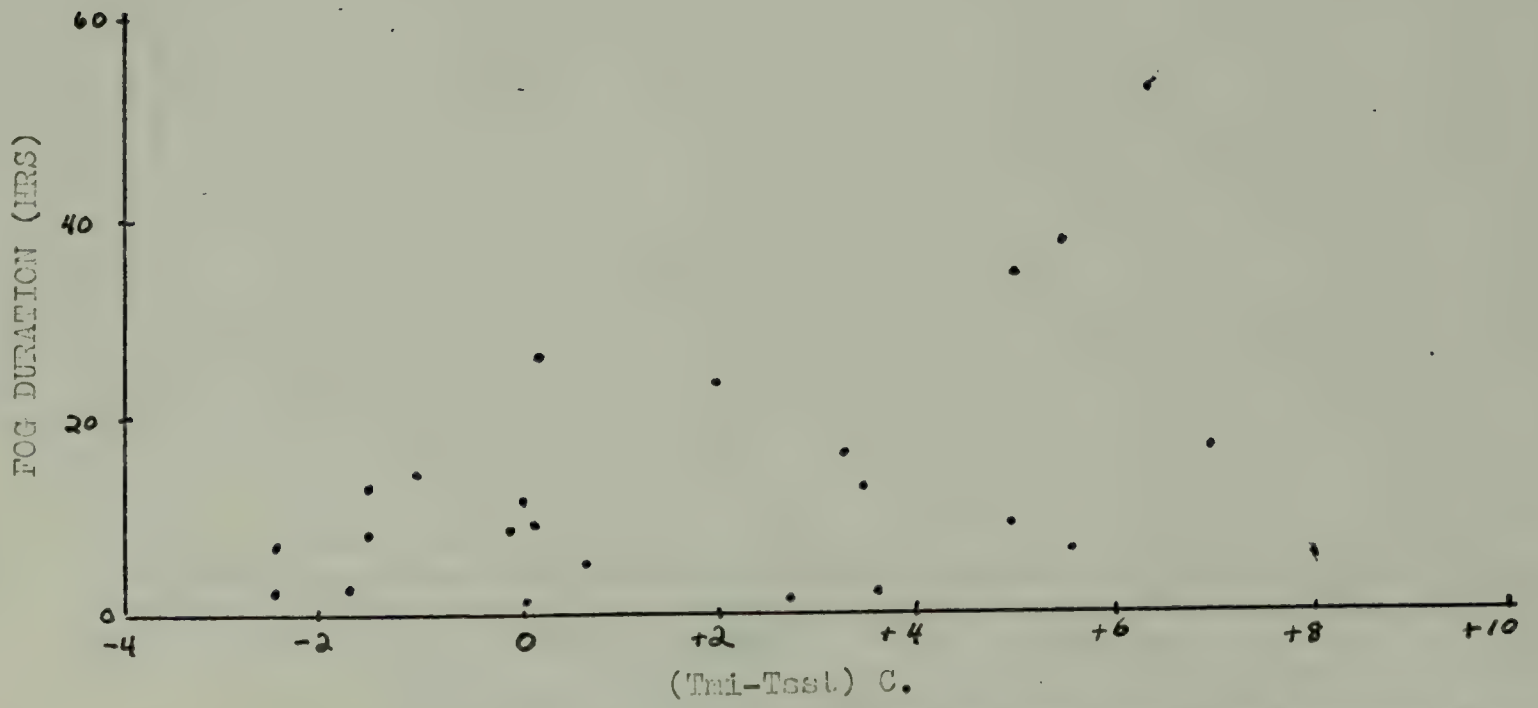

FOG DURATION VERSUS MAXIMUM SOUNDING TEMPERATURE MINUS SEA SURFACE TEMPERATURE

Q AND S

FIGURE 20

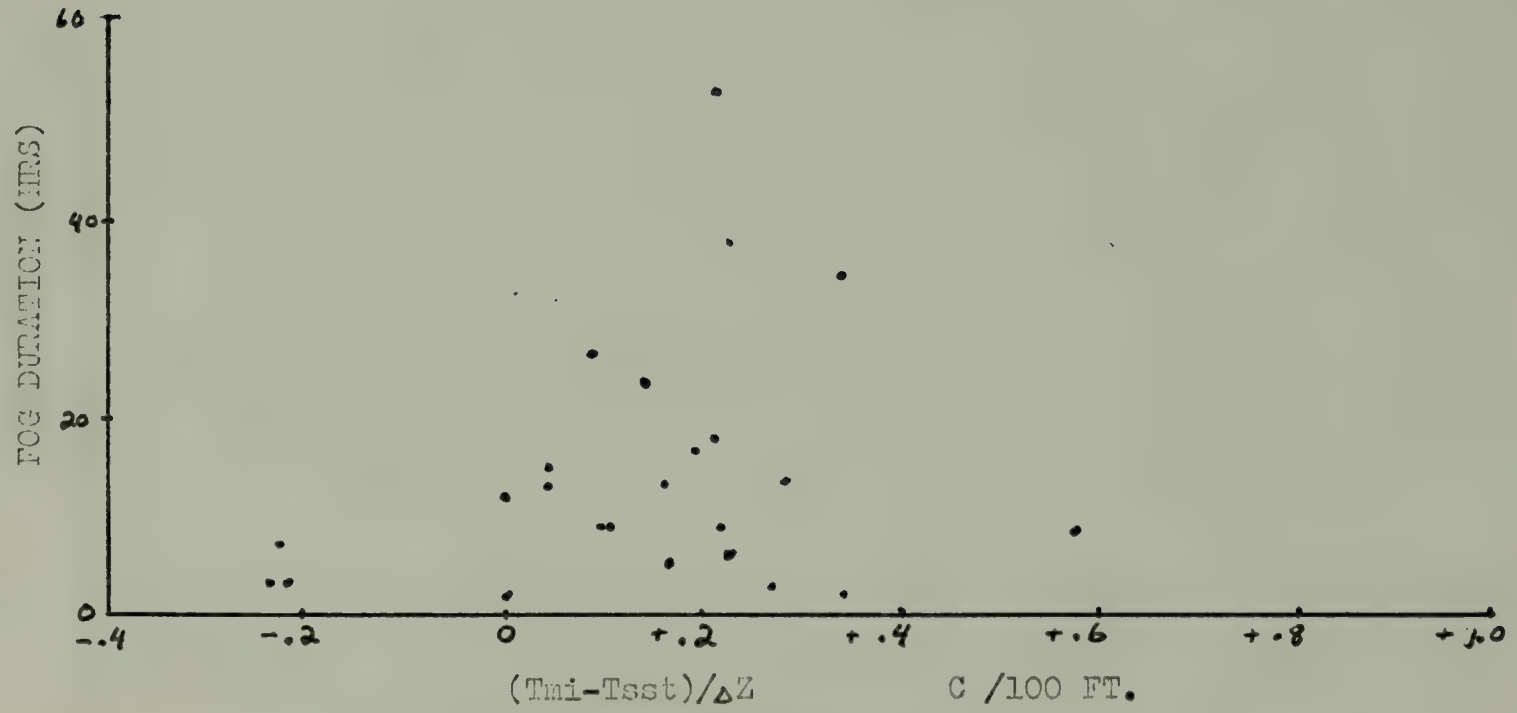

FOG DURATION VERSUS AVERAGE LAPSE RATE Q AND S

FIGURE 21

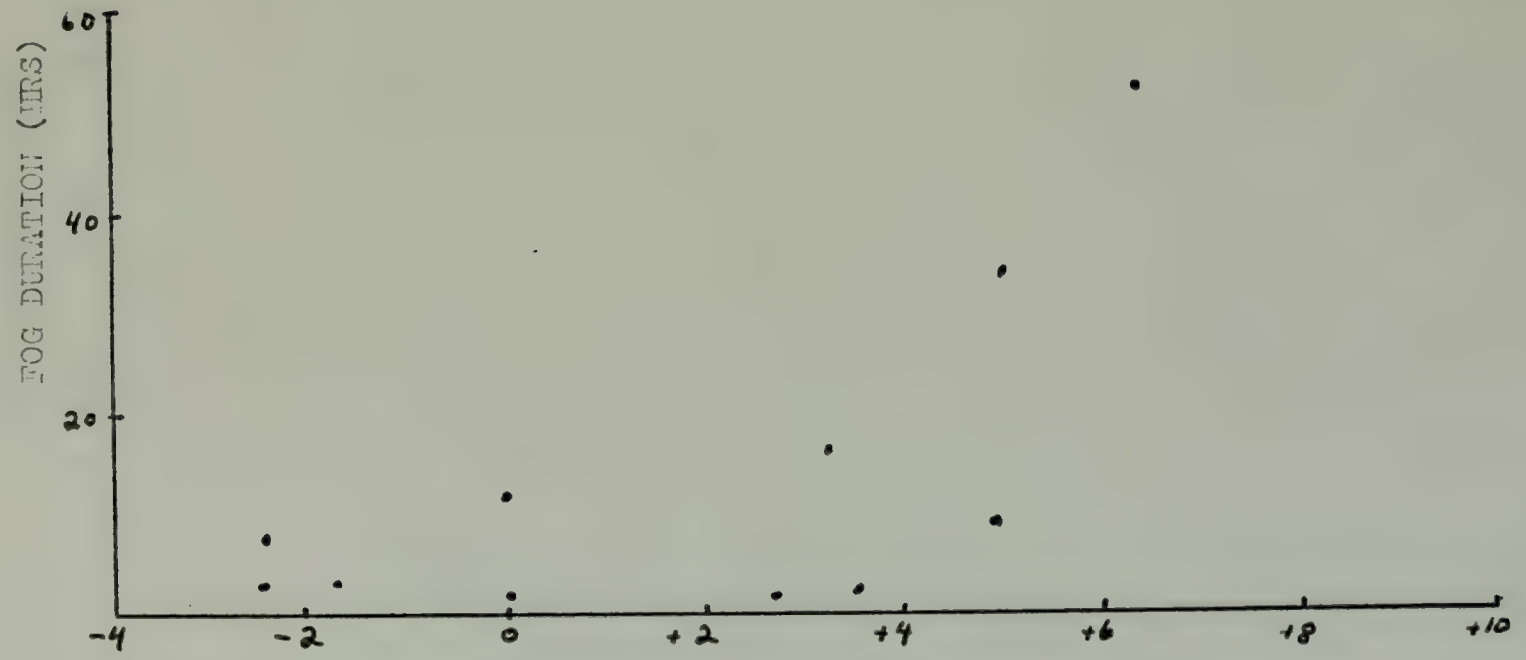

FOG DURATION VERSUS MAXIMUM SOUNDING TEMPERATURE MINUS SEA SURFACE TEMPERATURE

Q ONLY

FIGURE 22

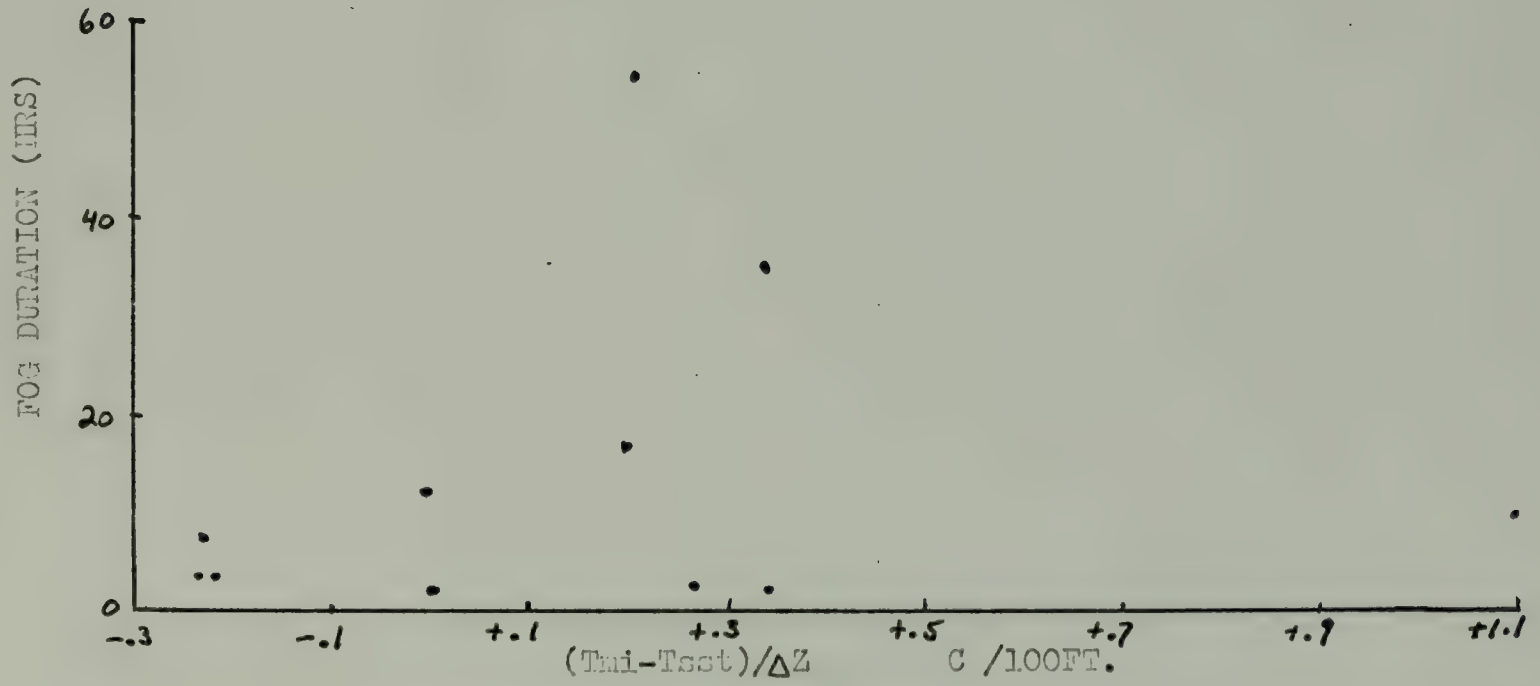

FOG DURATION VERSUS AVERAGE LAPSE RATE

Q ONLY

FIGURE 23

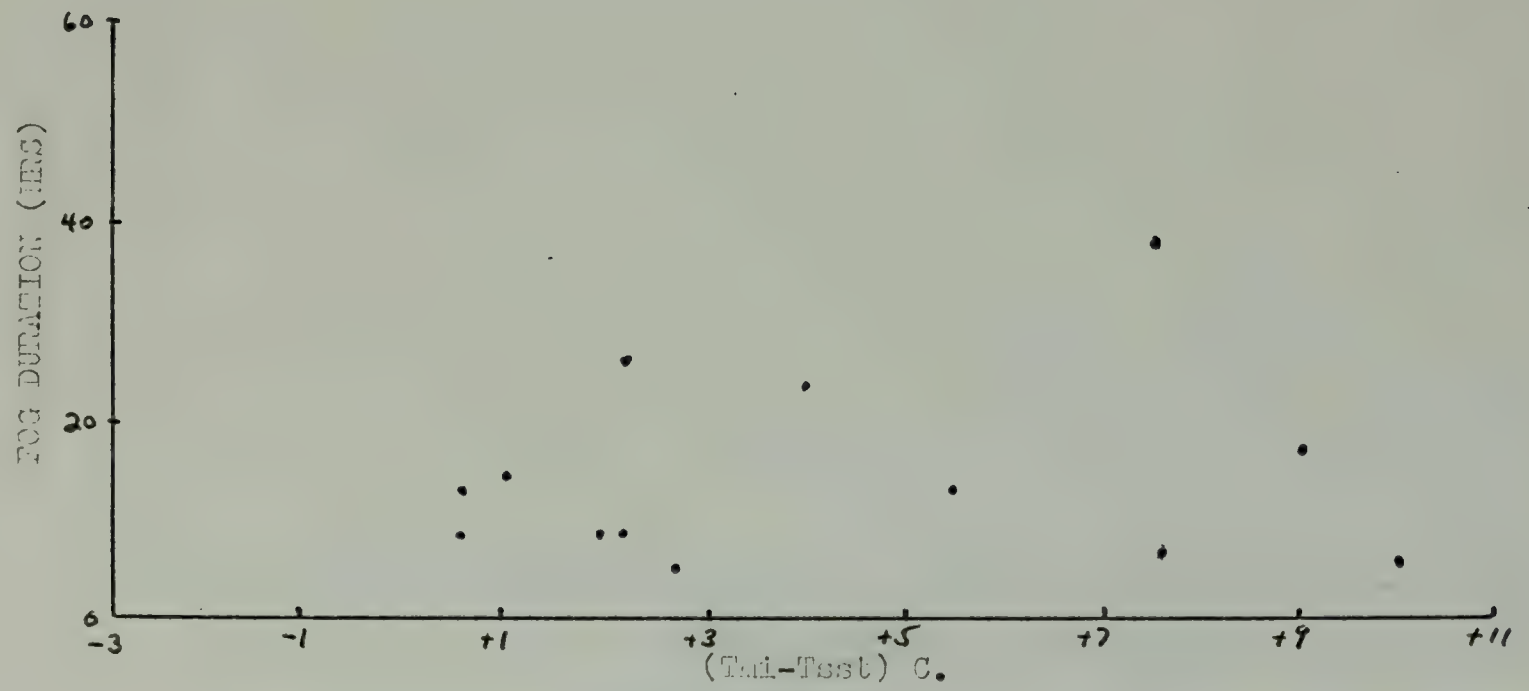

FOG DURATION VERSUS MAXIMUM SOUNDING TEMPERATURE MINUS SEA SURFACE TEMPERATURE

S ONLY

FIGURE 24

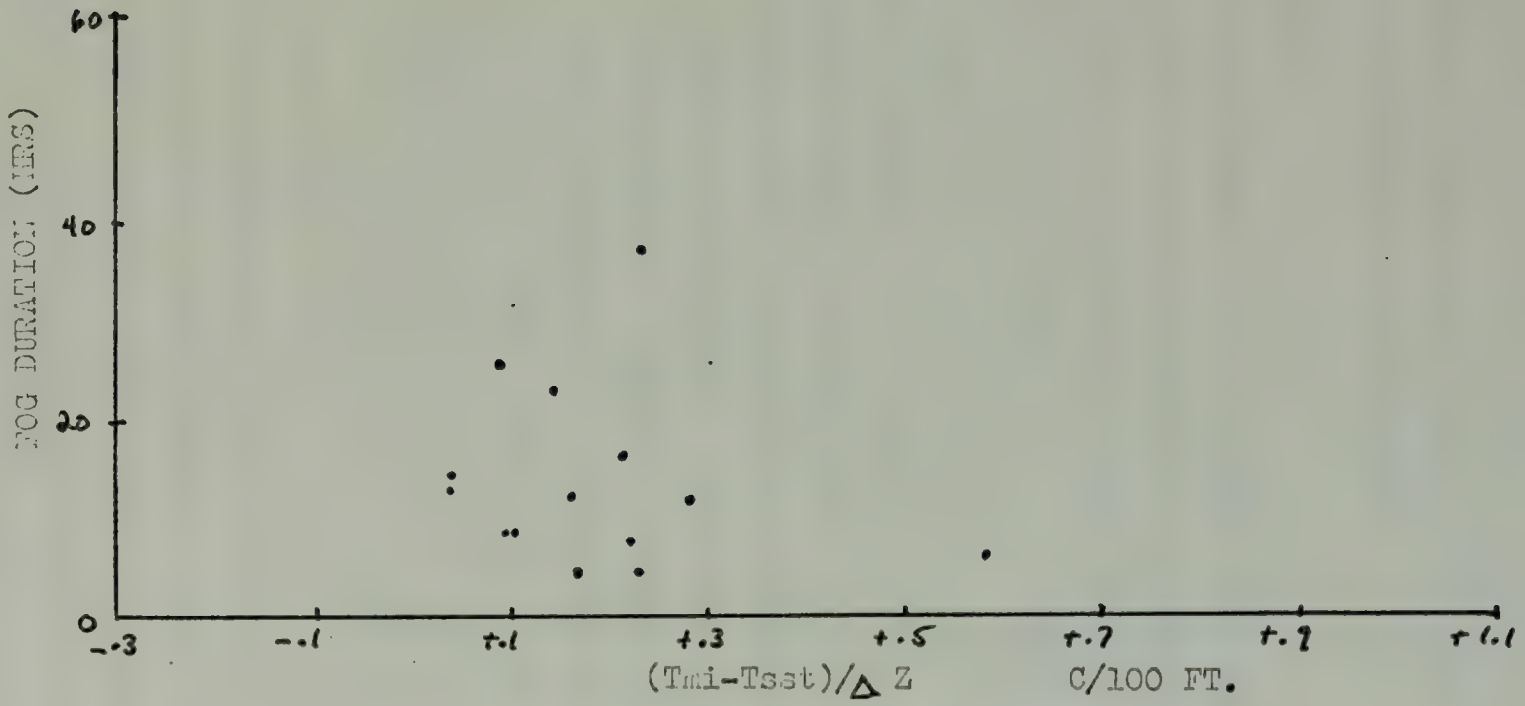

FOG DURATION VERSUS AVERAGE LAPSE RATE

S ONLY

FIGURE 25

The inversion relations are seen to be important both to the onset of fog as well as to the duration of the subsequent fog. The problem of forecasting the inversion boils down to being able to estimate a local heat budget including radiation effects on subsequent fogs which form.

C. SYNOPTIC RELATIONS

The interrelationship between fog occurrence and synoptic scale pressure systems were the last group of analyses considered. These analyses included the general circulation patterns which resulted in fog at each O.S.V. and the effects of the sea surface temperatures gradient upon the synoptic scale flow in fetches upstream of the fog occurrence.

The first investigation made was the effect of the storm tracks (paths which the centers of low pressure areas follow) on the occurrence of fog at each station. The dramatic increase in the number of fog cases in 1953 at each station from May to June was noted in Figure 13. To discern the reason for this difference, the storm tracks for May and June 1953 were determined and plotted in Figures 26 and 27 respectively. The dashed track represents the climatological storm track for the appropriate month [2]. It can be seen that while there is little change in the climatological storm track other than a somewhat more easterly track out from the Japanese Islands in June than in May, the particular tracks followed during May and June of 1953 differ noticeably. The main difference is in the branch of the cyclone track

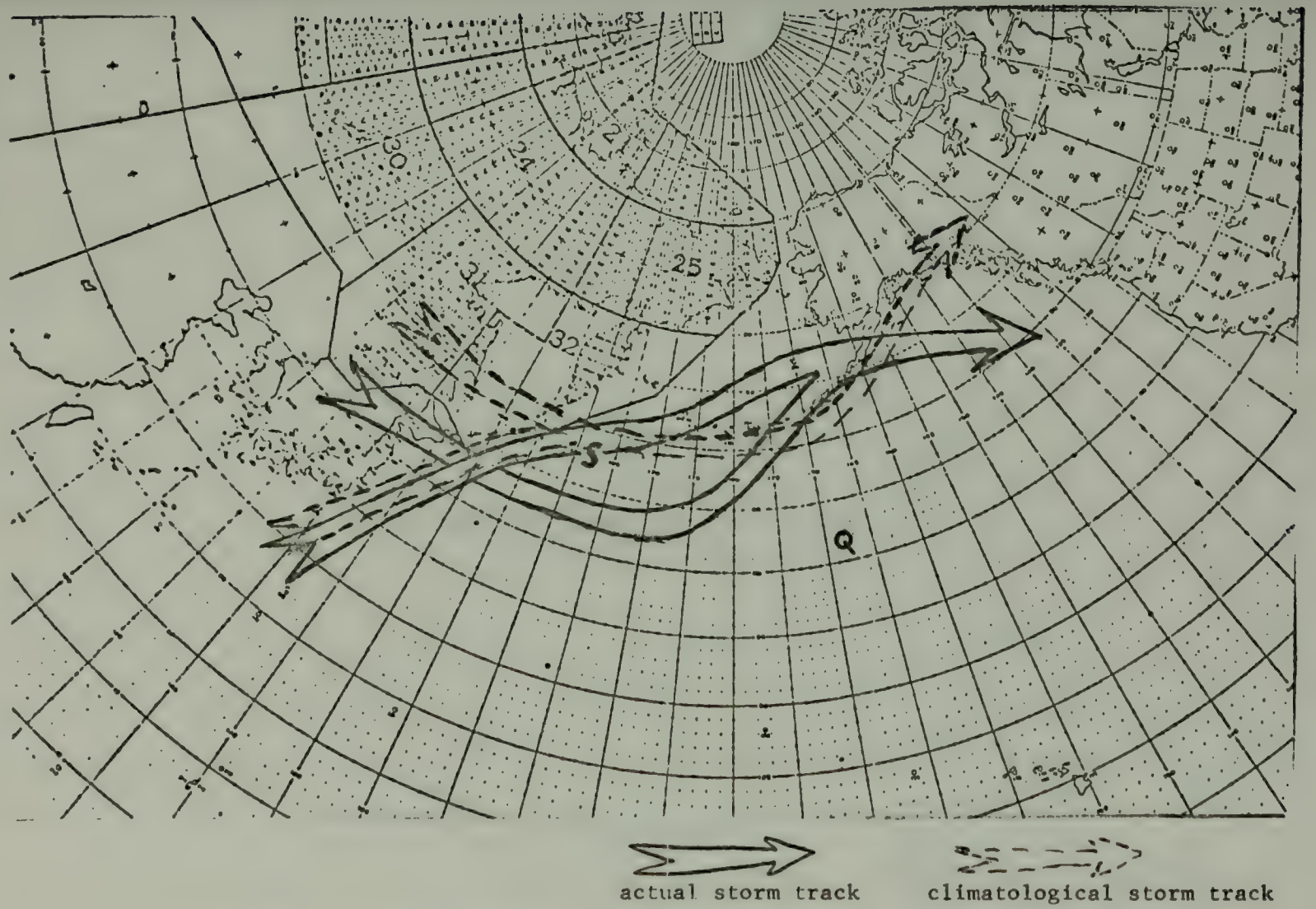

ACTUAL MAY 1953 STORM TRACKS AND MAY CLIMATOLOGICAL STORM TRACKS

FIGURE 26

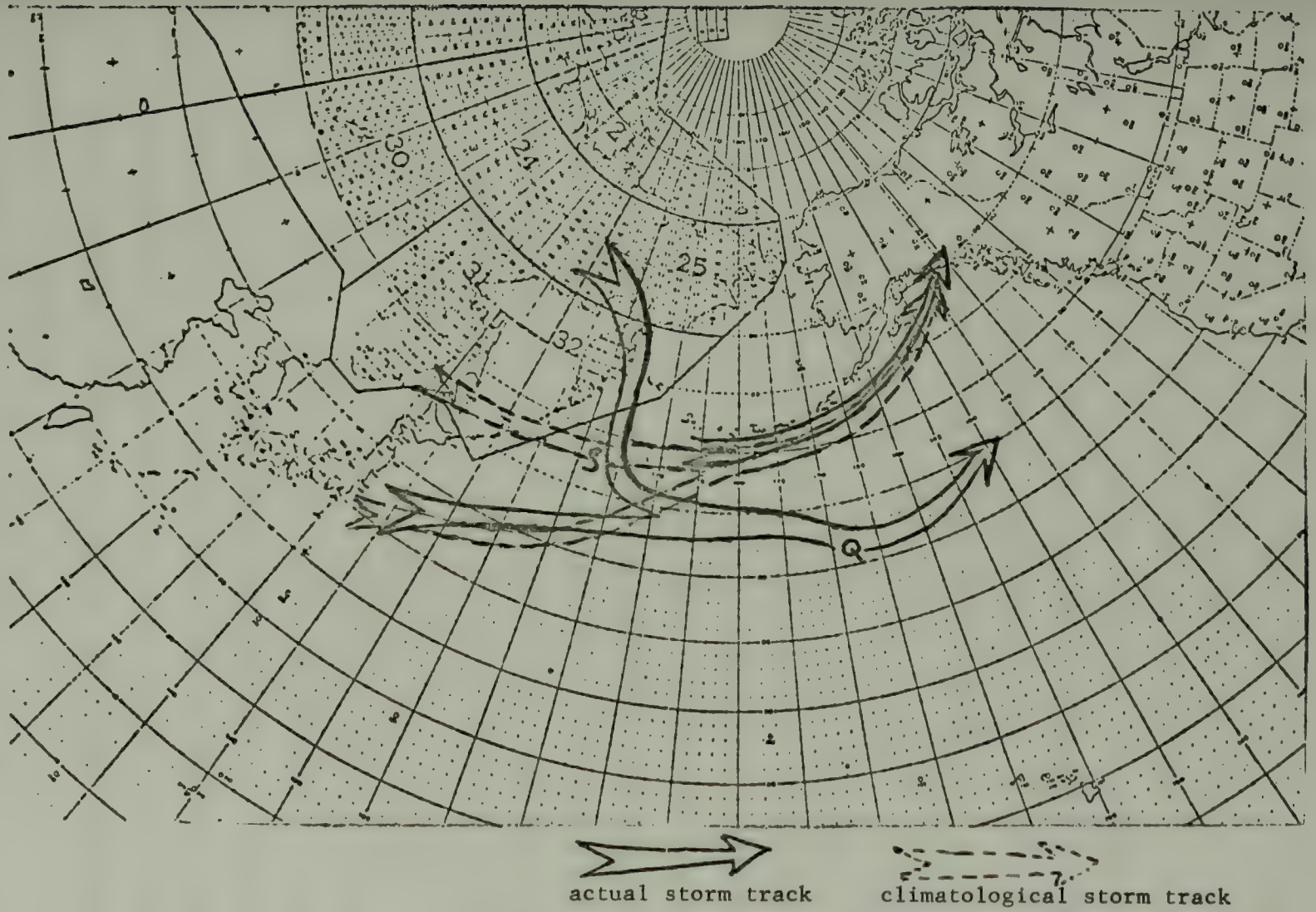

ACTUAL JUNE 1953 STORM TRACKS AND JUNE CLIMATOLOGICAL STORM TRACKS

FIGURE 27

coming out of Siberia. Since this particular track is not indicated in the climatology, it is difficult to determine whether the 1953 event is anomalous or not. It occurs during the time frame June 1-4 and again June 20-22. During both of these transits fog is evident at Station S, while at Q it is evident in the latter period. A data gap which occurred at Q during June 1-4 precludes knowledge of the conditions at the station during this time.

It is apparent that the track approaches Q much more closely in June than in May. The increased incidence of fog at Q may then be due to the closer approach of the tracks and the associated enhancement of advection from the south of warm moist air. At S, the northern approach of the cyclone centers in June ought to favor advection from the West Southwest across the station. This particular track might result in warm air being advected from the relatively warmer Sea of Japan into the Western North Pacific.

Studies of the synoptic conditions existing during the individual cases of fog at each station were made in an effort to determine those surface flow patterns which resulted in fog at the station. Figures 28-33 are a summary of the mean flow patterns observed prior to fog occurrence at each station. Each pattern was determined from the surface pressure maps of the daily synoptic map series, and represents the mean flow up to thirty six hours in advance of the fog occurrence.

Figure 28 shows a frontal fog occurrence at Station S with the trajectory of the air up from the south. What

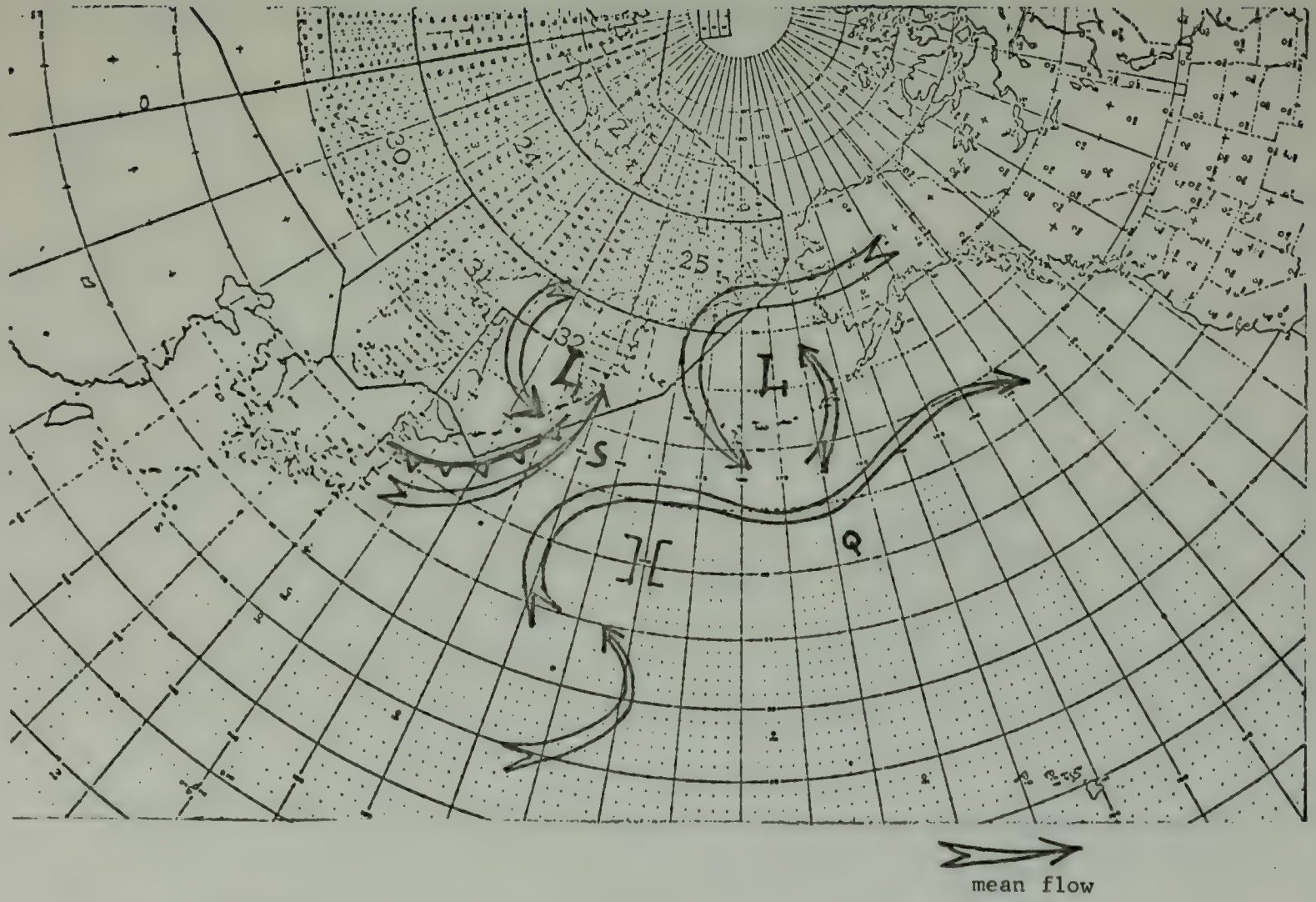

FLOW RESULTING IN FRONTAL FOG OCCURRENCE AT S, 7 MAY 1953

FIGURE 28

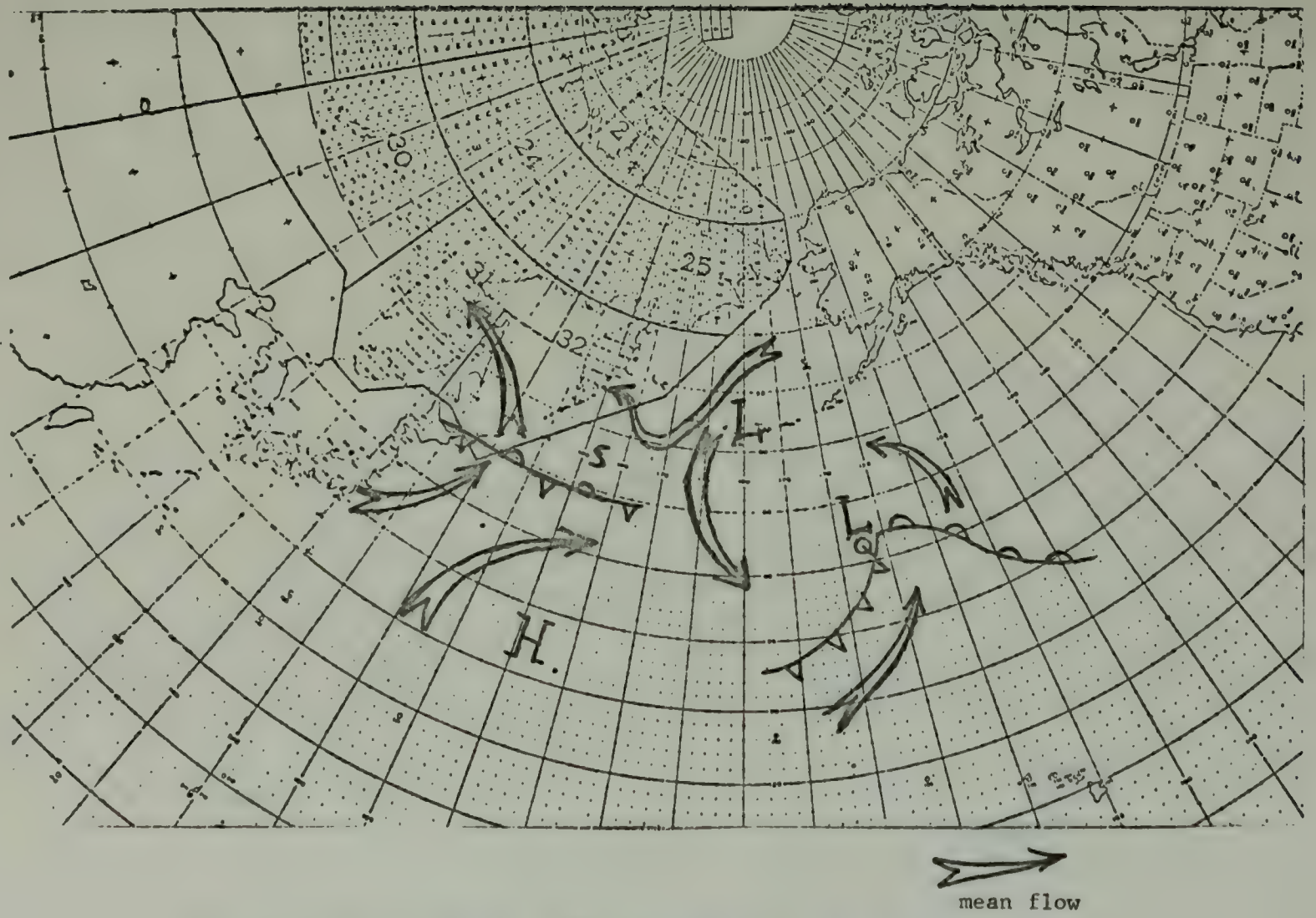

FLOW RESULTING IN FRONTAL FOG OCCURRENCE AT Q, 23 MAY 1953

FIGURE 29

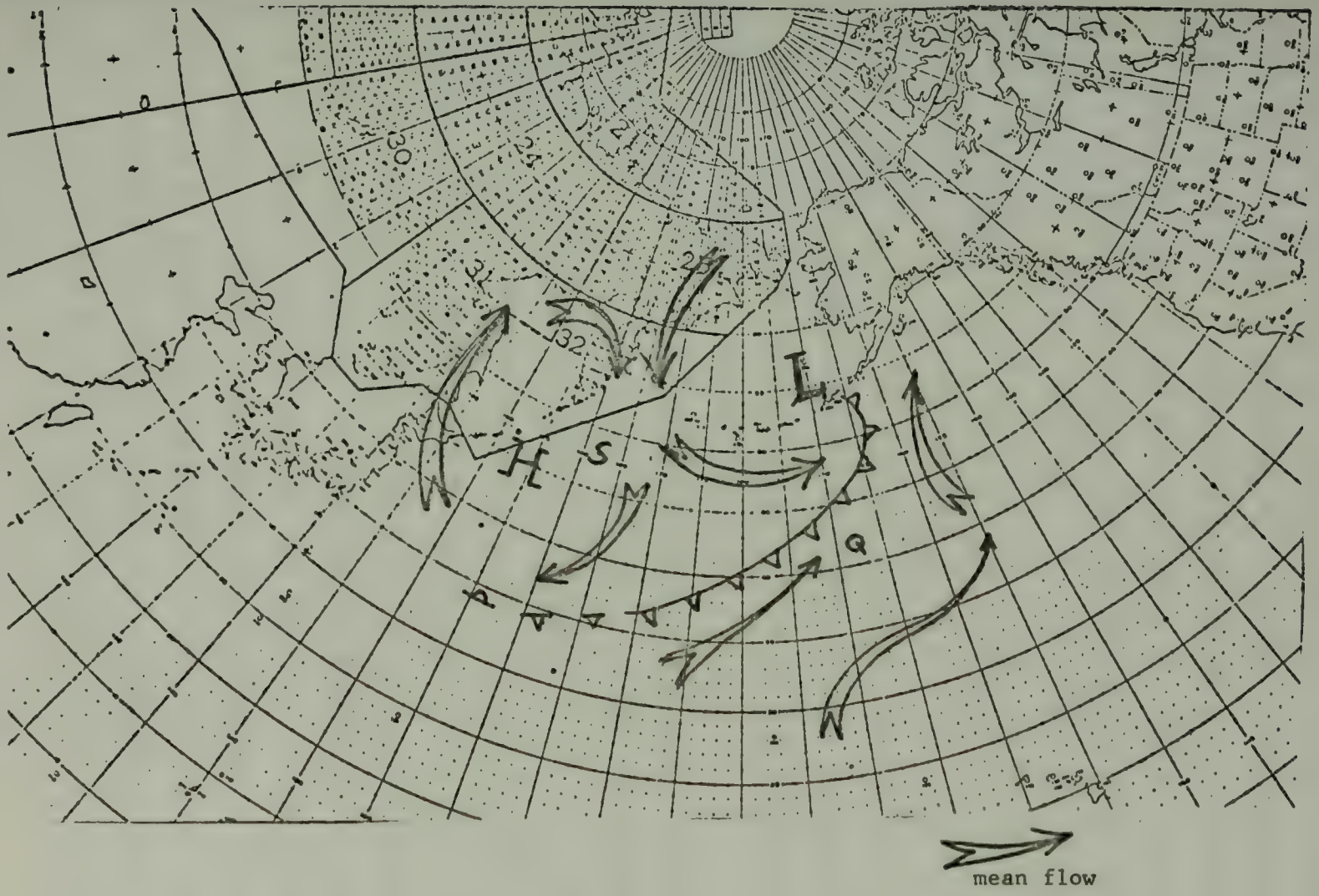

FLOW RESULTING IN AIRMASS FOGS AT Q AND S, 23 MAY 1953

FIGURE 30

distinguishes this case as frontal is that despite the advection of warm moist air from the south, frontal precipitation is also acting to increase the low level moisture content of the air at S. This case is actually a combination of frontal precipitation and advection effects. This particular flow resulted in two fog cases at Station S for a total duration of twenty hours.

Figure 29 is an example of a frontal fog occurrence at Station Q. It is evident that Q lies behind the cold front but quite close to the cyclone center. Precipitation again is mainly responsible here for maintaining moisture in the lower level and the resulting fog lasts for nine hours until drying finally dominates.

Figure 30 represents two airmass fog cases, one at S and the other at Q. Of particular note is the flow pattern at S since it is directly off the Kamchatka Peninsula. The temperatures of the air over the peninsula are higher in this case than the temperature of the sea surface between the peninsula and S. The result of this situation is an airmass fog with a northwesterly trajectory. At Station Q, although a front is in the proximity of the station, there is no precipitation effect at the station. The front is serving only as an impetus to southerly advection of warm air across the cooling sea surface temperature gradient. The duration of the fog at S is 14.5 hours divided into two cases, and at Q, 3.5 hours.

Figure 31 reveals a second airmass possibility at S with the flow around the low East Southeast of the Station

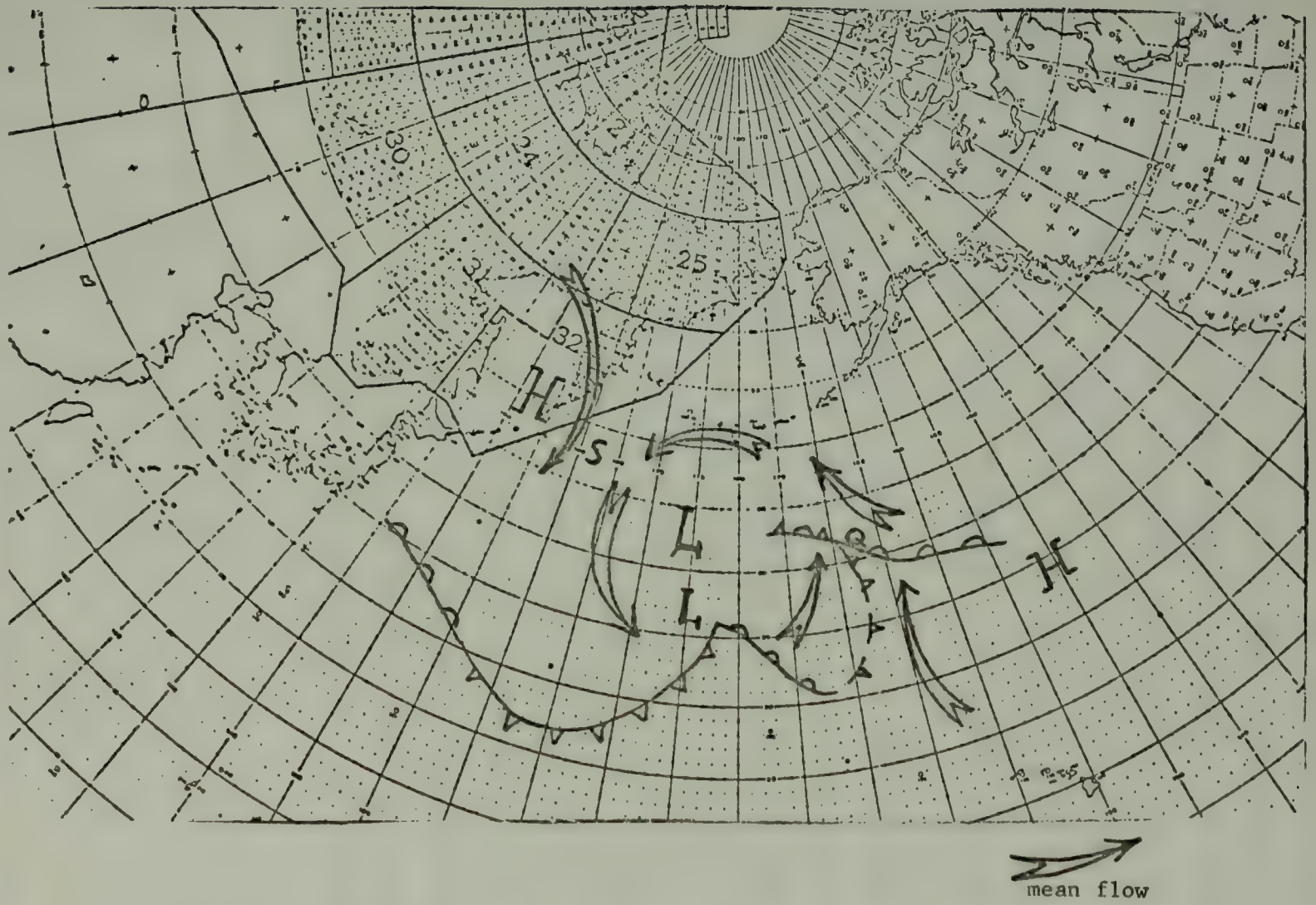

FLOW RESULTING IN FRONTAL FOG AT Q, AIRMASS FOG AT S, 7 JUNE 1953

FIGURE 31

supplying moisture to the station from the East. The flow is isothermal with regard to the sea surface isotherms, but the flow is originating in the southern latitudes, so as a result is still being subjected to cooling. At Station Q the fog case is again the result of a combination of frontal precipitation and warm air advection behind the warm front indicated. The duration of the resulting fog at Q is thirty-four hours, while at S the result is an eight and one-half-hour fog.

Figure 32 represents the case of fog occurring at Station S under conditions of a col. This case took place two days after the preceeding case described in Figure 31, and it is remarkable in that the resultant fog case shows the effects of radiational cooling described earlier in Section B of this chapter. The lack of any drying since the previous fog case meant that residual moisture was present in the low levels and upper level clearing conditions associated with the col permit the fog which is formed to radiate, thicken and persist for twenty hours. The fog itself is due initially to the moist flow coming around the low system to the East.

Figure 33 represents the final type of flow which results in fog at Station S. This flow is directly out of the Southern Sea of Okhotsk off the coast of China, across the Japanese mainland and directly out across S. This flow is directly off the warm near-shore waters of coastal Japan, across the Kuroshio Current, and over the colder water at Station S.

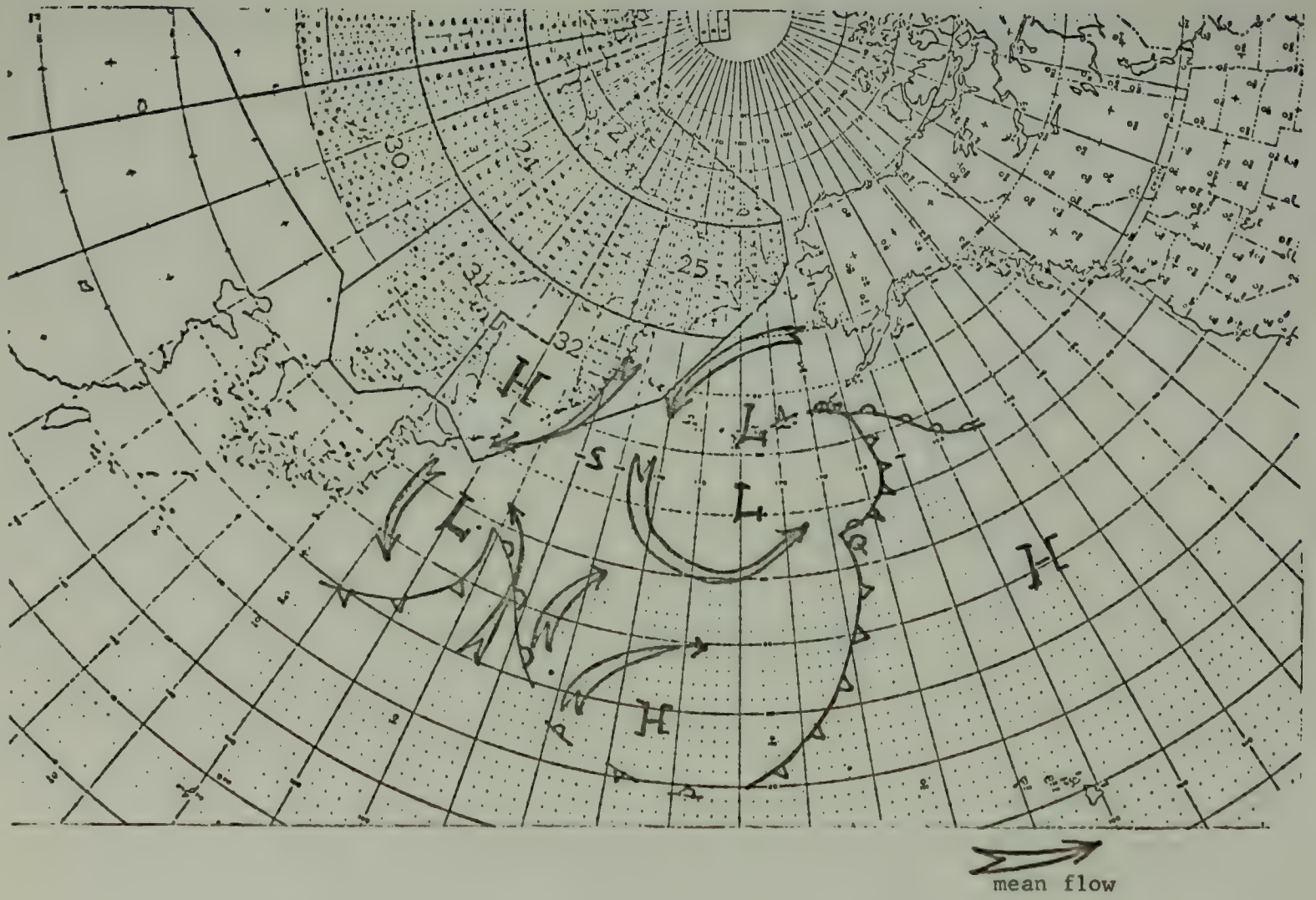

FLOW RESULTING IN AIRMASS FOG AT S, 9 JUNE 1953

FIGURE 32

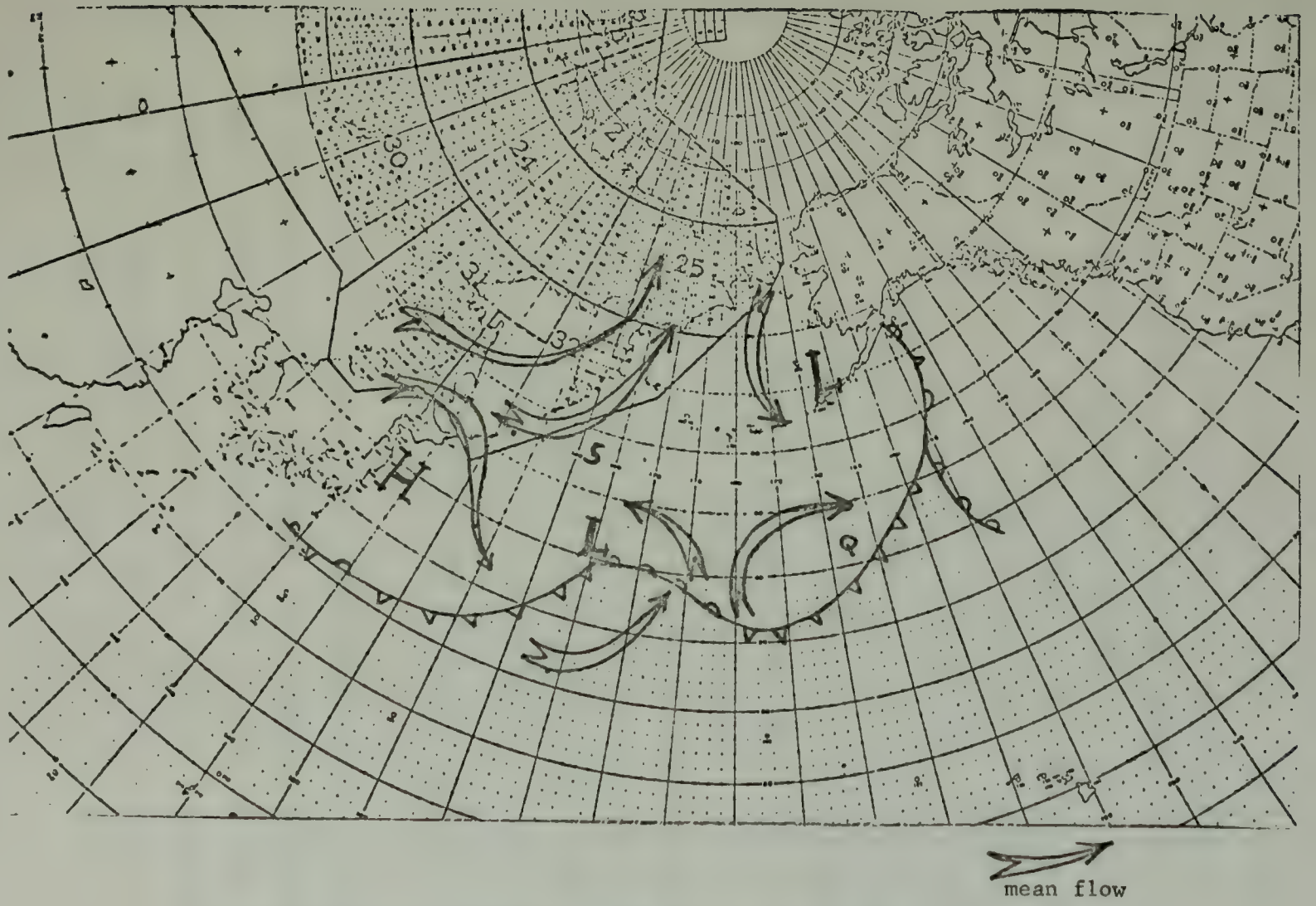

FLOW RESULTING IN OFFSHORE AIRMASS FOG AT S 13 JUNE 1953

FIGURE 33

This case, then represents the type of sea fog formed by cooling from below described by Taylor in the Grand Banks [17]. The resultant fog persists for 7.5 hours and is accompanied by drizzle associated with the thickening fog.

The preceeding series of figures demonstrates the types of flow associated with fog occurrence at Q and S. It was noted that except for the airmass fog at Station S due to offshore flow which is a special situation, those airmass cases at S with Northwest or Northerly station surface winds could all be related to the air originating in Southerly latitudes and coming up around high or low pressure systems. At Station Q the picture was much less complicated, with frontal and airmass fogs easy to delineate.

Pressure gradient studies of the fog cases were found to be inconclusive except in relation to associated winds due to the pressure gradient. The effect of these winds has been noted in Section A of this chapter, with the intense systems and attendant high winds making fog occurrence unlikely.

For those fog cases where fetches could be determined, an effort was made to determine the relation between cooling rate to which the air moving across the sea surface isotherms was being subjected and the duration of the resultant fog. This was accomplished through use of the ROMOT-MOSBY equation described earlier. In addition, the relationship between the size of the fetch as seen by a parcel of air transiting it and the resultant fog duration was examined. The relative

size of the fetch was expressed as a cooling duration. This quantity was obtained by dividing the fetch length by the mean wind velocity of the fetch.

Figure 34 is a plot of the cooling rate as determined by the ÅMOT-MOSBY formula versus the duration of the resultant fog case. The results are inconclusive, with data scatter great, however, it can be said that how fast cooling takes place has little relative effect on the duration of the subsequent fog. The cooling duration, on the other hand, appears to be related to the duration of the resultant fog as seen by the graph of Figure 35. The general trend is that the longer the cooling duration, the longer the resultant fog. The dashed line on the figure represents the approximate mean of the data points and the slope of the line is 0.385 indicating that fog duration for airmass fog cases with discernable fetches equals 0.385 of the cooling duration. Figure 35 concerns both Stations Q and S. In an effort to determine whether this relation held at each individual station, Figures 36 and 37 were constructed. Figure 36 summarizes those cases at Station Q and it can be seen that those two data points with the widest departure from the mean represent fog cases with a thick inversion present, as well as a positive (Td-Tsst). These very long duration fogs involve precipitation at the station intermittenly during the fog and this means that they have a combination of frontal and airmass characteristics which may explain the excessive duration of the fogs themselves. At

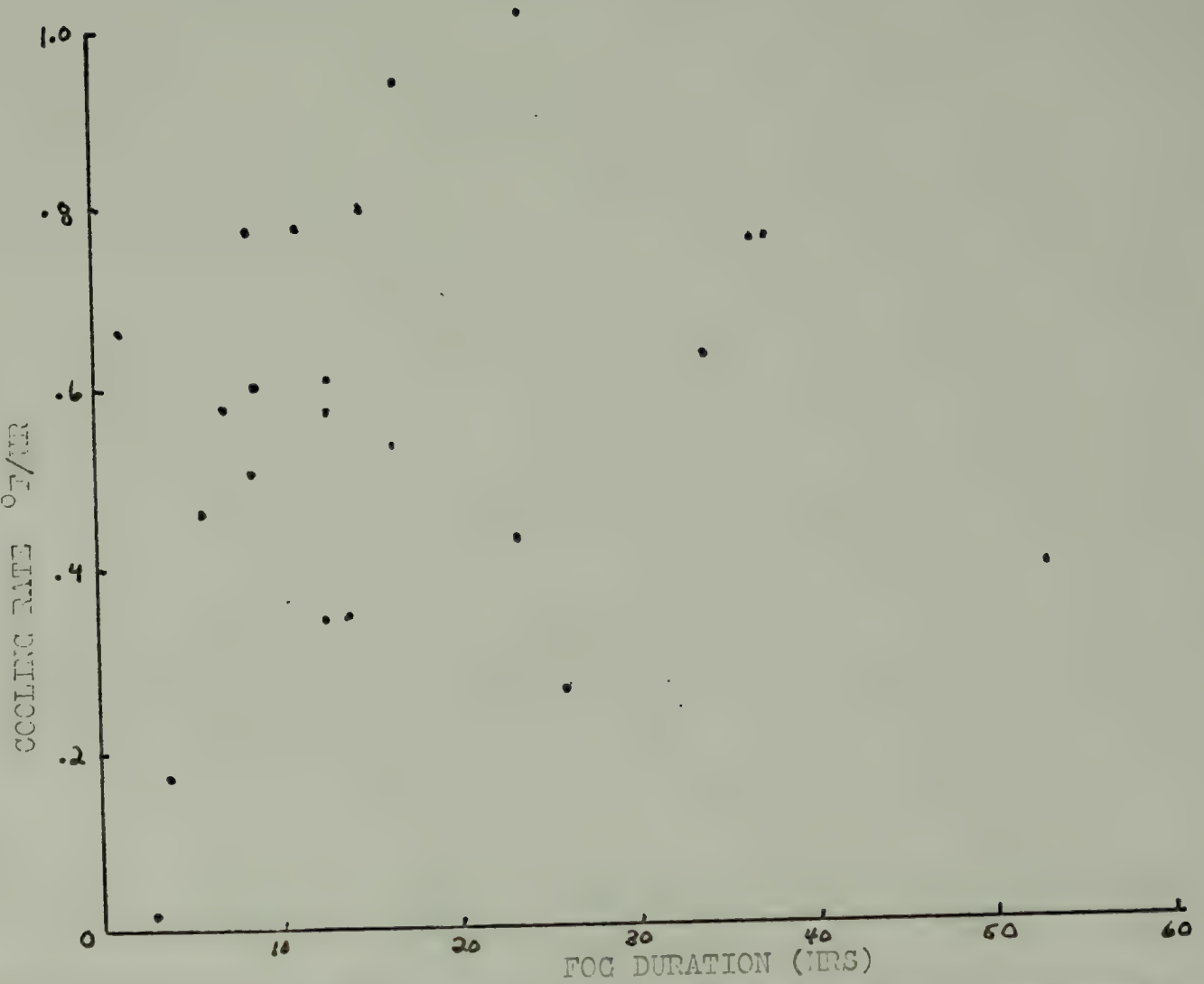

COOLING RATE VERSUS FOG DURATION FOR FOGS WITH FETCHES

FIGURE 34

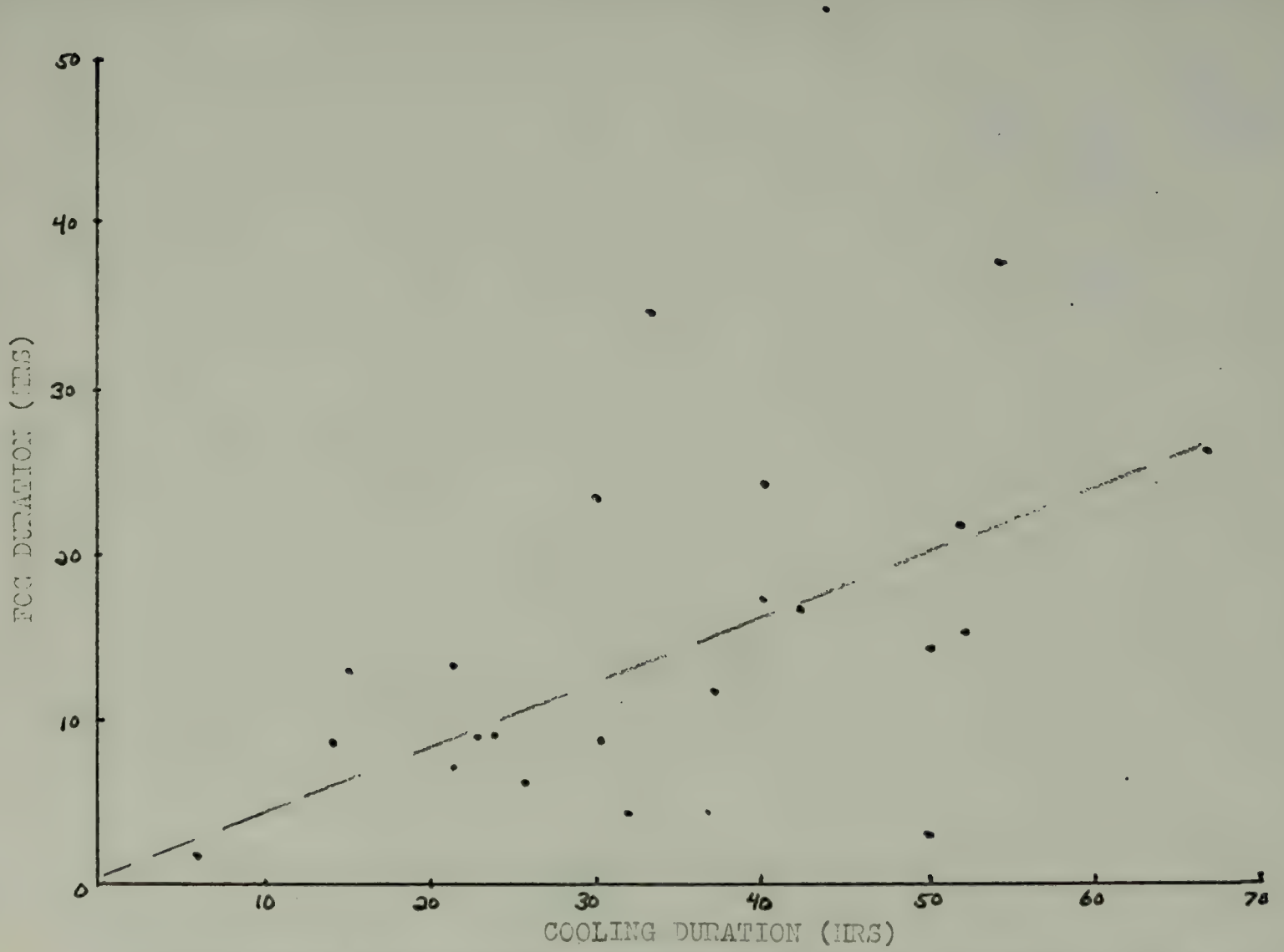

FOG DURATION VERSUS COOLING DURATION FOR FOGS WITH FETCHES BOTH Q AND S

FIGURE 35

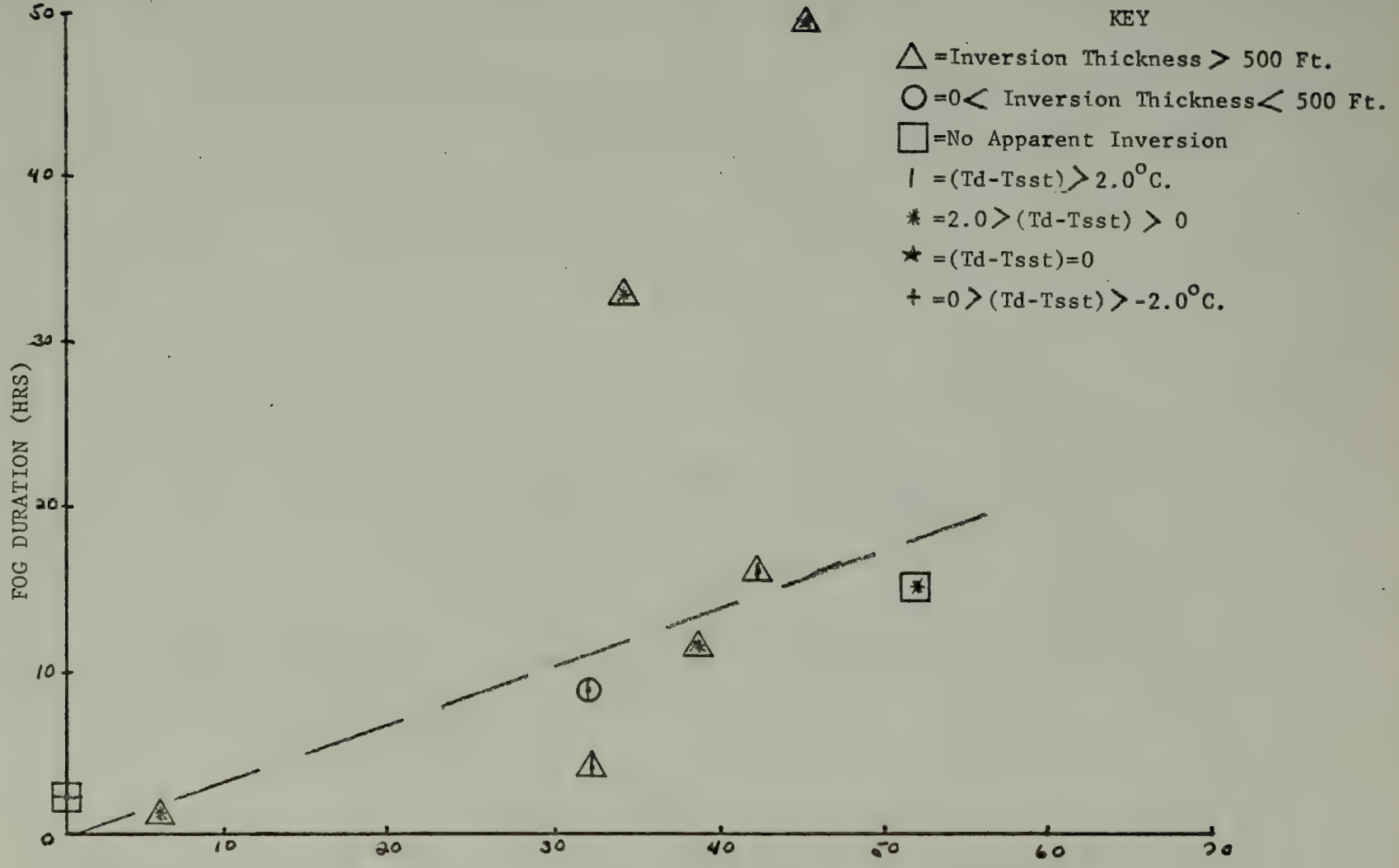

FOG DURATION VERSUS COOLING DURATION Q ONLY

FIGURE 36

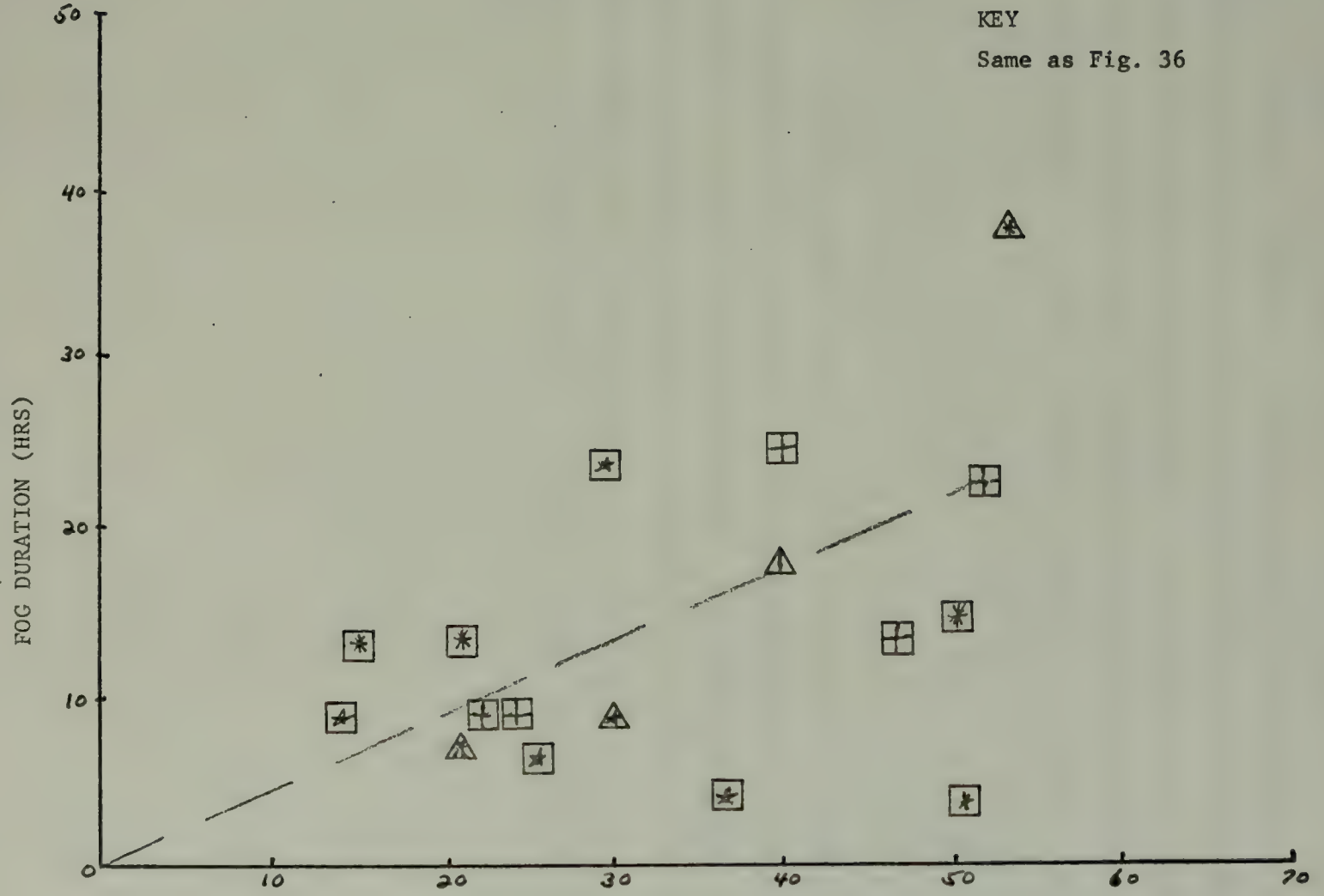

FOG DURATION VERSUS COOLING DURATION S ONLY

FIGURE 37

Station S the fit is better, as can be seen in Figure 37, with the greatest departures being one high duration case for long cooling duration and one short duration fog for long cooling duration. The selection of the fetch is the most subjective part of the analyses of airmass fogs and some scatter is undoubtedly due to the uncertainty inherant in fetch selection. Each fetch was selected on the basis of uniformity of wind orientation and speed within a sector of the pressure system under consideration. When two or more trajectories were indicated a mean fetch was constructed which was representative of the influence of each trajectory.

It would appear from this data that a useful handle in forecasting the duration of the fog resulting from advection of warm air from the south across a cooling sea surface temperature gradient is that the duration of the fog = 0.38 X the duration of cooling where the duration of cooling equals the fetch length divided by the mean wind velocity in the fetch.

VI. CONCLUSIONS

From the results of the preceeding chapter the following conclusions can be drawn concerning the occurrence of fog at ocean station vessels Quebec and Sierra during the months of May and June, 1953.

Fog occurrences at each station are associated with definite types of synoptic pressure systems and their accompanying air trajectories. Specifically, advection fogs occur at Station Q when warm moist air is advected across a cooling or isothermal sea surface temperature gradient. Advection fogs at Station S occur when the circulation pattern favors either the same case mentioned above, or when warm air advection from the Kamchatka Peninsula across the cooler North Pacific waters takes place. For those advection fogs where fetches were able to be determined the cooling duration of the air transiting the fetch was found to be related to the duration of the resulting fog by the relationship Fog Duration = 0.38 (cooling duration).

Frontal fogs can occur at both stations when precipitation falling from above causes saturation in an initially drier surface layer. This type of fog can occur either pre- or post-frontally and a forecast of its occurrence should be based on the humidity of the near surface marine layer and the response of the dewpoint in this layer to the precipitation falling from above.

Sea fog can occur at Station S when the air trajectory is off the Japanese Islands across the Kuroshio, from warm coastal water to the colder waters of the Northeast North Pacific. The absence of finely detailed surface isotherm patterns for this region during the time frame of the data prohibited the exact determination of cooling effects on the air trajectory in this case.

Three distinct inversion sequences are associated with the occurrence of fog at both stations. They are associated with the advection, frontal, and combined advection frontal effect fogs. The general rule determined for advection fogs is that the thicker the inversion, the longer the accompanying fogs will persist. In addition radiation effects were evident in the cooling of the fog to below the temperature of the sea surface during the inversion sequence.

Forecasting the inversion for advection cases will depend upon the ability to determine warm air advection in the surface to 750 mb. layer. The general tendency of fog to persist longer for those inversion cases with the greatest difference in maximum inversion temperature minus the sea surface temperature makes this ability desirable. The lack of intermediate layer data in the form of 850- and 700-mb. maps precluded an examination of advection above the surface. Forecasting the radiational effects on the existing fog requires a knowledge of the atmosphere thermal structure and the cloudiness above the fog to determine the likelihood and efficiency of the radiative processes.

The evaluation of point meteorological parameters revealed that the ability to locally forecast the dewpoint relative to the sea surface temperature as a measure of moisture content and the air temperature minus the dewpoint as a measure of the saturation of the air are critical to any fog forecast.

Results indicated that when the (Ta-Td) separation is greater than 2.0C. fog will not occur, and further, if the (Ta-Td) separation is less than 0.5C. fog will occur 93% of the time at these stations. The dewpoint-sea surface temperature separation is a useful indicator in predicting those cases for which no fog will be expected. This is when the dewpoint is more than 2.5C. below the sea surface temperature.

The effect of the wind speed upon the occurrence or non occurrence of fog was seen to be usable in forecasting no-fog cases based on an upper limit cut off speed of 30 knots. Since the wind speeds are a function of the gradients existent in the surface pressure field, the use of such gradients in determining wind velocities is indicated. The occurrence of fog was found to be independent of the value of the station pressure existent at the time of formation, but it was found that fog occurrence was less likely in rising pressure situations than in steady or falling pressure regimes, leading to the conclusion that vigorous post frontal passages lead to no-fog forecasts.

The initial visibility of the fog was found to be generally related to the wind speed and the (Ta-Td) separation. As a rule, the higher the wind speed the greater the initial

visibility and the higher the separation of (Ta-Td), the greater the initial visibility. Data scatter precluded a definite determination of any objective relation.

From the standpoint of fog prediction utilizing point parameters such as air temperature, dewpoint, and wind direction and speed alone, it was found through rate of change studies that the greatest amount of change in these parameters prior to fog formation occurs in the time frame of six hours prior to the onset of the fog. For extremely short term forecasting the time series analysis technique would be useful, but long-range fog forecasting is beyond the capability of this technique when used alone.

A procedure for making a fog forecast in the vicinities of the two North Pacific Ocean Stations studied might be based on the following:

A. Advection Fogs

1. Evaluate the synoptic scale pressure patterns to determine areas of warm air advection across cooling or isothermal sea surface temperature gradients.
2. Estimate the magnitude of the warm air advection in relation to the sea surface temperature for areas in A-1.
3. Determine a fetch from the existing and progged pressure maps, within which wind direction and speed with relation to the sea surface isotherms are approximately constant, and determine the cooling duration of the air within the fetch.

4. Forecast the wind conditions in the area being considered to see if fog formation will be possible, i.e. wind speeds less than 30 kts.
5. Determine the rate of convergence of the air temperature and the dewpoint in the area upwind of the fetch to forecast the onset time of the fog.
6. Use #2 and #3 to determine the duration of the resulting fog.

B. Frontal Fogs

1. Determine areas in frontal zones where precipitation is falling into drier surface layers which are warmer than the sea surface.
2. Determine the rate of change in the moisture content of the surface layer to determine a fog onset time.
3. Determine the rate of drying behind the frontal zone to forecast a dissipation time.

C. Sea Fogs

1. Determine areas where trajectories of the wind will be from areas of relatively warm water to cooler water.
2. Determine a cooling duration in the same manner as A-3 above.

This rather simplistic outline in itself is valid if all the steps can be accomplished. The problem lies in the accomplishment. Fetch determination is highly subjective, advection and evaporation moisture changes fall into the realm of complex heat budget determinations, and the status

of present atmospheric models is such that useful determinations of specific values for thermal advection cannot be made remotely for specific locations with the degree of accuracy required for carrier operations for example.

In the outline above, however, this paper has demonstrated that some of the steps can indeed be accomplished. For airmass fogs, in step A-1, areas of warm air advection can be estimated from surface pressure maps well enough to determine areas of high fog probability of occurrence.

Utilization of radiosonde information, when available, can enable step A-2 to be accomplished through the inversion relationships described earlier. Although exact numerical values cannot be determined, this step will enable a judgement to be made as to whether the ensuing fog will be of short or long duration.

If a clear cut fetch is determinable, step A-3 can be used to estimate the duration of the subsequent fog via the relationship Fog Duration = 0.38 (cooling duration). Low level wind forecast techniques presently in use are accurate enough to enable this estimation to be made. Additionally, step A-4 can be accomplished via the same wind forecasts mentioned above.

As was mentioned earlier, the rate change studies indicate that a short term accomplishment of step A-5 is possible. Short term here means up to nine hours in advance of the onset of fog. Although an exact method of forecasting a precise start time is not presented by this step, it is possible for a shipboard forecaster, for example, to narrow

down his estimate of when the fog is likely to start by observing the rates of change of the temperature and dewpoint in his operations area.

For frontal fogs, step B-1 can be accomplished if radiosonde data is available in such areas, hence its accomplishment is limited to ships which take radiosonde soundings on a routine basis and which are operating in frontal areas.

Steps B-2 and B-3 may be accomplished in some measure by again observing the time rates of change of the dewpoint as a measure of the moisture content of the air.

For sea fogs in section C, the same comments apply as those for sections A-1 and A-3.

As this paper has demonstrated, time series analyses of observations made by shipboard meteorologists can be employed in conjunction with synoptic pressure maps to determine short range fog forecasts during at-sea operations. Until numerical fog models can achieve accurate results on a point basis, it seems that shipboard fog forecasts must be made on the following basis: A combination of Synoptic reasoning and those point and synoptic statistics which have been put forth in this paper.

VII. RECOMMENDATIONS FOR FURTHER STUDY

The following recommendations for further study are listed below:

A. Acquire better data. The analytical techniques used in this paper were extremely data limited and these limitations are as follows.

1. Surface observations were taken at three-hour intervals, necessitating the assumption of linear changes between succeeding observations.
2. Historical synoptic maps were available at twenty four hour intervals only, again necessitating assumptions of continuity in pressure system movements and air trajectory determinations.
3. Initial conditions at the upwind edge of fetches were difficult to obtain.
4. Exact sea surface temperature gradients for the months of May and June 1953 were unavailable, necessitating the use of climatological means.
5. Upstream radiosonde data was lacking.
6. Synoptic maps on the intermediate levels between the surface and 750 mb. levels were unavailable.

The analysis techniques would have been enhanced greatly had the above factors been alleviated. The availability of continuous weather observations from fixed oceanic points is, however, limited to the observations taken by the Ocean Station Vessel observation program and, as a result, the

use of this data is restricted to the time period during which these vessels were active. One solution to the aforementioned limitations would be a modern effort to couple a surface synoptic observation system, such as automated weather buoys, with the satellite capabilities being promised in the future. Satellites with the ability to obtain a temperature sounding profile of the atmosphere are almost within reach and this system coupled with ocean surface observations and existing hemispheric numerical wind and pressure pattern prognoses would go a long way toward alleviating many of the difficulties mentioned previously. In view of the lack of such a system at present, another possible technique would be to utilize a combination of ships and aircraft capable of investigating the temperature structure of the atmosphere via the use of radiosondes and dropsondes. Also, measurements of sea surface temperature gradients could be made via the use of airborne radiometers.

B. Expand the scope of the investigation. Although the deficiencies enumerated above exist, much additional data covering months of 1953 not analyzed in this study, as well as months from other years remains available. This data should be analyzed through the combined techniques of synoptic analyses and fixed point time series to determine the applicability of the results of this paper to fog occurrence throughout the North Pacific, and to fog occurrence during the other months of the year as well.

C. Thermal and radiation data should be employed to determine the local heat budgets for operational areas. The effects of radiation cooling on fogs in the open ocean could be better understood by a more thorough understanding of the total heat budget in the area.

D. Numerical models of fog are under development and refinement at the present time by various individuals and agencies. The development should continue and the surface observations taken by the O.S.V. stations should be utilized to provide real data in these theoretical models to aid in their development toward operational applicability.

In conclusion, the problem of forecasting fog in the open ocean is one of accumulation of sufficient information concerning the mechanisms of formation, persistence, and dissipation. It is this accumulation of data which has been the stumbling block to marine fog forecasting techniques in the past.

BIBLIOGRAPHY

1. Byers, H. R., General Meteorology, McGraw Hill, 1959.

2. Crutcher, H. L., and Davis, O. M., U. S. Navy, Commander Naval Weather Service Command, (NAVAIR50-1C-54) Marine Climatic Atlas of the World, V. 8, 1 March 1969.

3. Gathman, S. G., and Larson, R. E., "Marine Fog Observations in the Artic," NRL Report 7693, April 8, 1974.

4. Grisham, P. O., and Renard, R. J., An Investigation of Marine Fog Formation and Occurrence Over the North Pacific Ocean Area, Research Paper, U. S. Naval Postgraduate School, September, 1973.

5. Laevastu, T., and Carstensen, L. P., Numerical Analysis and Forecasting of Surface Air Temperature and Water Vapor Pressure, U. S. Naval Fleet Weather Facility, Technical Note No. 17, April 1966.

6. Laviolette, P. E., and Seim, S. E., Monthly Charts of Mean, Minimum, and Maximum Sea Surface Temperature of the North Pacific Ocean, SP 123, Naval Oceanographic Office, 1969.

7. Leipper, D. F., "Fog Development at San Diego, California," Sears Foundation: Journal of Marine Research, V. 7, No. 3, p. 337-346, November 15, 1948.

8. Leipper, D. F., "The Sharp Smog Bank and California Fog Development," Bulletin of the American Meteorological Society, Vol. 49, No. 4, p. 354-358, April 1968.

9. Leipper, D. F., Forecasting Summer Fog at Shemya, Operational Forecast Paper, Weather Central Alaska, 11th Weather Region, AAF, 1 June 1945.

10. Nelson, T. S., Numerical-Statistical Prediction of Visibility at Sea, M. S. Thesis, U. S. Naval Postgraduate School, 1972.

11. Ogata, T., Kanazawa, M., and Yoshida, F., "The Sea Fog Over the Open Sea," Kishocho Kenkyu Jiho, Journal of Meteorological Research, Tokyo, V. 10, p. 253-259, 1958.

12. Ogata, T. and Tamura, Y., "The Sea Fog Over the Open Sea," Kishocho Kenkyu Jiho, Journal of Meteorological Research, Tokyo, part 1, V. 7, p. 633-642, 1955.

13. Renard, R. J., Research Activities on Analysis and Prediction of Marine Fog, Paper, U. S. Naval Postgraduate School, 1974.

14. Roll, J. U., Physics of the Marine Atmosphere, Academic Press, 1965.

15. Schramm, W. G., Analysis and Prediction of Visibility at Sea, M. S. Thesis, U. S. Naval Postgrate School, 1966.

16. Stevenson, R. E., "The Summer Fogs Along the Yorkshire Coast, England," Essays in Marine Geology in Honor of K. O. Emery, University of Southern California Press, 1963.

17. Taylor, G. I., "The Formation of Fog and Mist," Quarterly Journal of the Royal Meteorological Society, V. 43, p. 241-268, 1917.

18. U. S. Navy Weather Research Facility, Meteorological Probabilities for Planning Carrier Task Force Operations in the North Pacific, NWRF 09-0662-061, Norfolk, Virginia, June 1962.

19. U.S. Weather Bureau, Daily Series Synoptic Weather Maps Part 1, Northern Hemisphere, U. S. Department of Commerce, 1953.

20. Wheeler, S. E., The Impact of Marine Fog on Naval Operations, M. S. Thesis, U. S. Naval Postgraduate School, 1974.

21. Willet, H. C., "Fog and Haze," Monthly Weather Review, V. 56, p. 435-467, 1928.

INITIAL DISTRIBUTION LIST

		No. Copies
1.	Department of Oceanography, Code 58 Naval Postgraduate School Monterey, California 93940	10
2.	Oceanographer of the Navy Hoffman Building No. 2 200 Stovall Street Alexandria, Virginia 22332	1
3.	Office of Naval Research Code 480 Arlington, Virginia 22217	1
4.	Dr. Robert E. Stevenson Scientific Liaison Office, ONR Scripps Institution of Oceanography La Jolla, California 92037	1
5.	Library, Code 3330 Naval Oceanographic Office Washington, D.C. 20373	1
6.	SIO Library University of California, San Diego P. O. Box 2367 La Jolla, California 92037	1
7.	Department of Oceanography Library University of Washington Seattle, Washington 98105	1
8.	Department of Oceanography Library Oregon State University Corvallis, Oregon 97331	1
9.	Commanding Officer Fleet Numerical Weather Central Monterey, California 93940	1
10.	Commanding Officer Environmental Prediction Research Facility Monterey, California 93940	1

11.	Department of the Navy Commander Oceanographic System Pacific Box 1390 FPO San Francisco 96610	1
12.	Defense Documentation Center Cameron Station Alexandria, Virginia 22314	12
13.	Library (Code 0212 Naval Postgraduate School Monterey, California 93940	2
14.	National Center for Atmospheric Research Library Aquisitions Boulder, Colorado 80301	1
15.	Dr. James L. Kassner, Jr. Graduate Center for Cloud Physics Research University of Missouri, Rolla, Missouri 65401	1
16.	Naval Weather Service Command Naval Weather Service Headquarters Washington, D. C. 20390	1
17.	Air Weather Service (AWVAS/TF) Scott AFB, Illinois 62225	1
18.	Department of Meteorology, Code 51 Naval Postgraduate School Monterey, California 93940	1
19.	Dr. Robert J. Renard, Code 51 Department of Meteorology Naval Postgraduate School Monterey, California 93940	1
20.	Prof. Charles L. Taylor, Code 51 Department of Meteorology Naval Postgraduate School Monterey, California 93940	1
21.	Dr. Glenn W. Jung, Code 58 Department of Oceanography Naval Postgraduate School Monterey, California 93940	1
22.	Dr. Dale F. Leipper, Code 58 Department of Oceanography Naval Postgraduate School Monterey, California 93940	1 1

23. Capt. Frank J. Misciasci, Jr. — 2
PSC Box 853
APO New York 09406

24. Dr. Alan Weinstein — 1
Stratiform Cloud Physics Fr.
Meteorology Laboratory
Department of the Air Force
Air Force Cambridge Res. Lab.
Laurence G. Hanscom Field
Bedford, Mass. 01730

25. Dr. Pierre St. Amand — 1
Earth and Planetary Sci. Div.
Code 602
Department of the Navy
Naval Weapons Center
China Lake, California 93555

26. Mr. Murray H. Schefer — 1
AIR-370C
Naval Air Systems Command
Washington, D. C. 20360

27. Dr. Lothar Ruhnke — 1
Naval Research Laboratory
Washington, D. C. 20390
Code 8320

28. Dr. Patrick Squires — 1
Desert Research Institute
University of Nevada
Reno, Nevada 89507

29. Dr. Thomas E. Hoffer — 1
Desert Research Institute
University of Nevada
Reno, Nevada 89502

30. Mr. James Hughes — 1
Office of Naval Research
Code 412
Arlington, Virginia 22217

31. Mr. Paul R. Lowe — 1
Environmental Prediction Research
Facility
Naval Post Graduate School
Monterey, California 93940

32. Mr. Edward Barker — 1
Environmental Prediction
Research Facility
Monterey, California 93940

33. Mr. Roland Pilie — 1
Calspan Corporation
Buffalo, New York 14221

34. Dr. Dee F. Taylor — 1
Naval Air Systems Command
AIR-540
Washington, D. C. 20360

Thesis
M6365 Misciasci
c.1
155452
Fog occurrence and forecasting at two North Pacific ocean stations, May and June, 1953.